Inverse Problems in Systems Biology

Heinz W. Engl

Johann Radon Institute for Computational and Applied Mathematics, Austrian Academy of Sciences, Altenbergerstraße 69, 4040 Linz, Austria

E-mail: `heinz.engl@oeaw.ac.at`

Christoph Flamm

Institute for Theoretical Chemistry, University of Vienna, Währingerstraße 17, 1090 Wien, Austria

E-mail: `xtof@tbi.univie.ac.at`

Philipp Kügler

Industrial Mathematics Institute, Johannes Kepler University Linz, Altenbergerstraße 69, 4040 Linz, Austria

E-mail: `philipp.kuegler@jku.at`

James Lu

Johann Radon Institute for Computational and Applied Mathematics, Austrian Academy of Sciences, Altenbergerstraße 69, 4040 Linz, Austria

E-mail: `james.lu@oeaw.ac.at`

Stefan Müller

Johann Radon Institute for Computational and Applied Mathematics, Austrian Academy of Sciences, Altenbergerstraße 69, 4040 Linz, Austria

E-mail: `stefan.mueller@oeaw.ac.at`

Peter Schuster

Institute for Theoretical Chemistry, University of Vienna, Währingerstraße 17, 1090 Wien, Austria

E-mail: `pks@tbi.univie.ac.at`

Abstract. Systems biology is a new discipline built upon the premise that an understanding of how cells and organisms carry out their functions cannot be gained by looking at cellular components in isolation. Instead, consideration of the interplay between the parts of systems is indispensable for analyzing, modeling, and predicting systems' behaviour.Studying biological processes under this premise, systems biology combines experimental techniques and computational methods in order to constructpredictive models. Both in building and utilizing models of biological systems, inverse problems arise at several occasions,for example, (i) when experimental time series and steady state data are used to construct biochemical reaction networks, (ii) when model parameters are identified that capture underlying mechanisms or (iii) when desired qualitative behaviour such as bistability or limit cycle oscillations is engineered by proper choices of parameter combinations.In this paper we review principles of the modelling process in systems biology and illustrate the ill-posedness and regularization of parameter identification problems in that context. Furthermore, we discuss the methodology of qualitative inverse problems and demonstrate how sparsity enforcing regularization allows the determination of key reaction mechanisms underlying the qualitative behaviour.

Keywords. Systems biology, parameter identification, qualitative inverse problems, reverse engineering, biochemical reaction networks, bifurcation pattern, sparsity

1. Introduction and motivation

Systems biology is a relatively young biological discipline that claims to consider cells and organisms as entities in a holistic way. At the same time it focuses on the interplay of components from the molecular to the systemic level. Quantitative measurements and recordings of biological processes are merged with advanced mathematical methods to yield predictive theoretical, mostly computational, models of biological systems. In this sense systems biology introduces quantitative mathematical modeling into biology and bridges thereby the gap between experimental and theoretical scientific methods. The systems concept as such is not new and has already been approached long ago in physiology, for example in modeling drug effects in medicine through pharmacokinetics and pharmacodynamics, see, e.g., [129].

The experimental data base for systems biology comes from various high-throughput technologies applied in fields usually ending in "-omics". These experimental technologies provide a global "snapshot" of particular cellular processes, such as gene expression or metabolism, at a defined instant. For example all transcripts present in a cell – termed the transcriptom – can be characterized simultaneously using for instance DNA microarrays. Transcriptomics aims at the exploration of the transcriptom and how it varies with cell type, stage of development or environmental conditions. Metabolomics, in addition, deals with the quantification of the time dependent composition of the set of organic molecules that constitutes cellular metabolism. Included in the metabolism are the enzymes that catalyze the interconversion of metabolites. In other words, the metabolism of the cell is the set of several thousands of catalyzed biochemical reactions resulting in molecular concentrations of a large number of substrates, products and enzymes as functions of time. Data collection, data validation and model building are the great challenges of systems biology for essentially two reasons:

(i) The almost one hundred years old conventional approach to dynamical phenomena at the molecular level in biology is biochemical kinetics. It provides accurate rate parameters determined under precisely defined conditions for *in vitro*

assays. The transfer of these parameters to the conditions within living cells is anything but trivial. Moreover, the fraction of rate parameters that was directly determined by rigorous physical methods is rather small compared to the set of all parameters needed in systems biology.

(ii) On the experimental side, present-day high-throughput technologies may reflect directly the situation in the cell but are "snapshots" and allow for conclusions on processes only if they can be repeated at sufficiently high frequency. Most of the reliable information from current microarrays provide only qualitative – "yes" or "no" – or at best semi-quantitative – "0", "1", ..., "n" – data that have to be converted into numerical quantities in order to be a useful basis for parameter estimation. Data collected in this way are usually quite noisy, which is a special challenge for the inverse problem of determining parameters; the mathematical methods to be used for this purpose are a major topic in this review paper.

In order to create a sufficiently large data pool, systems biology requires simultaneous experimental approaches like biochemical kinetics, microarray data harvesting, and other techniques, for example time resolved high-resolution spectroscopy. Efficient and optimal, the synergy of different techniques exploiting tools are not yet available but under fast progressing development, see, e.g., [87,108].

The success of biochemical kinetics on enzyme reactions *in vitro* is certainly responsible for the overwhelming fraction of biological models that are based on ODEs. For physicists and chemists it would be desirable to use mass action kinetics on the elementary step level. The complexity of biological signalling and reaction networks, however, is prohibitive for the complete treatment and simplifications have to be used. The conventional approach to enzyme catalyzed reaction, for example, is Michaelis-Menten kinetics that subsumes the reaction steps of an enzyme reaction under a single over-all reaction. Similarly, many-step polymerization reactions as they occur in replication, transcription, and translation may be represented by appropriate approximations through single-step reactions. Ignoring initial reaction phases allows for the assumption of steady states and again reduces the number of reaction steps and the number of variables in the over-all kinetics.

One of the major goals of systems biology is to provide an understanding of properties and behavior of cells or organisms emerging as consequence of the interaction of large numbers of molecules, which organize themselves into highly intricate reaction networks that span various levels of cellular or organismal complexity. The number of nodes in metabolic networks amounts to several thousand molecules. To illustrate this complexity by means of an example, the bacterial cell of the species *Escherichia coli* has 4 460 genes giving rise to roughly the same number of transcripts and translation products. The cell is robust against changes in the surrounding and collects information on the environment. The chemical reactions within the cell form a highly organized network controlled by a genetic regulatory system. The available experimental data are far from being complete in the sense that they cover all cellular processes and therefore highly involved techniques are required to extract as much information as possible from experiment and to identify parameters that are crucial for system behavior. A higher level of complexity concerns, for example, the organization of the human body with approximately 20 000 genes and 200 different cell types.

Here we present an overview on the application of inverse problem solving methods to questions of systems biology. In particular, we shall distinguish two different classes of problems: (i) *parameter estimation* from experimental data sets and (ii) *qualitative inverse problems* that aim at reverse engineering of bifurcation patterns and other types of desired qualitative behavior. Parameter estimation commonly

aims at one of two goals: It provides values or at least upper and lower bounds for unknown or difficult to determine parameters. Alternatively, it is important to know insensitivities of data sets to certain parameters, which then are not accessible from the given data and require additional experimental information for their determination. Related to this problem is the question of sparsity in the reaction matrix: Which are the parameters and the reaction variables that are strongly coupled and essential to obtain the observed data? Inverse problems of that type are discussed in Sections 2.2 and 3.1. Qualitative inverse problems are used to explore the areas in parameter space that give rise to a given qualitative behavior, e.g., multiple steady state solutions, oscillations, deterministic chaos, etc. Typical engineering questions are: Which are the parameters that maximize or minimize a stable closed orbit? An example is given in Section 3.2. How can the bifurcation pattern of a given reaction network be influenced by changing certain parameters? A practical implication would be, for example, the determination of parameter sets that arrest the cell cycle of given cell types in a certain phase and prohibit malignant proliferation thereby. How can one adjust the circadian rhythm such that it responds fast and smoothly to a pace maker reset in order to avoid negative consequences of jet lag? We come back to inverse problems for circadian rhythms in Section 3.2.3.

2. Computational systems biology

In biology, a broad collection of measuring techniques ranging from single-molecular fluorescence based methods to techniques that measure mean values over whole cell populations (such as microarray and sequencing technology which characterizes gene expression or mass spectroscopy which allows for access to metabolite levels) is applied to collect the relevant data sets. In many cases the entities of interest must be first "extracted" from the complex cellular matrix by multi-step experimental protocols before they are amenable to quantification, thereby making it hard for one to make general statements about the "typical" data error present in systems biology data sets. Furthermore, some of the experimental techniques provide information only at a qualitative or semi-quantitative level. To cope with noise, measurement errors and missing data points, which are typical issues for biological data, in building system biology models one would have to integrate experimental data from diverse sources [119].

Depending on the quality of the biological data available a wide variety of mathematical modeling approaches have been applied in systems biology. Often, biological data is only available at a qualitative level. A good example for this type of data are protein interaction networks [3]. Proteins are capable of interacting with each other in a highly specific manner which can be formally represented by a graph. However, in many cases the strength of interaction (graph edges) and the precise composition of protein interaction complexes (graph nodes) are unknown. Nevertheless, the analysis of the network topology of these types of cellular networks have uncovered important functional organisation principles [8] and underlying design principles [2]. Metabolic networks, which consist of enzyme catalyzed reactions that transform organic molecules for the purpose of acquiring energy and constructing complex compounds used in cellular functioning, are among the best studied networks in biology. Although the topology of these networks and the exact stoichiometry (i.e. the quantitative relationship between reactants and products) of the individual chemical reactions are well known, only little information is available on the functional form and the kinetic parameters of the enzymatic rate laws. This lack of information renders the large scale modeling of the metabolite
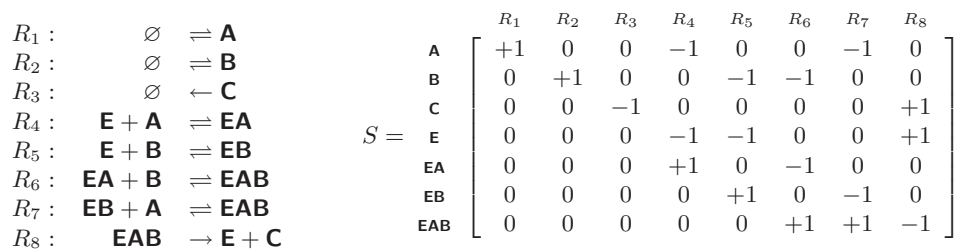
$$
\begin{array}{ll}
R_1: & \varnothing \rightleftharpoons \mathbf{A} \\
R_2: & \varnothing \rightleftharpoons \mathbf{B} \\
R_3: & \varnothing \leftarrow \mathbf{C} \\
R_4: & \mathbf{E}+\mathbf{A} \rightleftharpoons \mathbf{EA} \\
R_5: & \mathbf{E}+\mathbf{B} \rightleftharpoons \mathbf{EB} \\
R_6: & \mathbf{EA}+\mathbf{B} \rightleftharpoons \mathbf{EAB} \\
R_7: & \mathbf{EB}+\mathbf{A} \rightleftharpoons \mathbf{EAB} \\
R_8: & \mathbf{EAB} \rightarrow \mathbf{E}+\mathbf{C}
\end{array}
$$

$$
S = \begin{array}{c|cccccccc}
 & R_1 & R_2 & R_3 & R_4 & R_5 & R_6 & R_7 & R_8 \\
\hline
\mathbf{A} & +1 & 0 & 0 & -1 & 0 & 0 & -1 & 0 \\
\mathbf{B} & 0 & +1 & 0 & 0 & -1 & -1 & 0 & 0 \\
\mathbf{C} & 0 & 0 & -1 & 0 & 0 & 0 & 0 & +1 \\
\mathbf{E} & 0 & 0 & 0 & -1 & -1 & 0 & 0 & +1 \\
\mathbf{EA} & 0 & 0 & 0 & +1 & 0 & -1 & 0 & 0 \\
\mathbf{EB} & 0 & 0 & 0 & 0 & +1 & 0 & -1 & 0 \\
\mathbf{EAB} & 0 & 0 & 0 & 0 & 0 & +1 & +1 & -1
\end{array}
$$

Figure 1. Representation of a chemical reaction network as chemical equations (left) and as stoichiometric matrix (right). The equations describe the mechanism for an enzyme catalyzed reaction with unordered substrate binding which is found in the cycline-dependent kinase-catalysed phosphorylation reaction at the heart of the cell cycle. This example network is discussed in more detail in Appendix A.

concentrations and their rates of change in terms of ODEs impossible. However, the varying (mass)fluxes through the metabolic network depend on the laws of chemistry which constrain the supply and demand of metabolites within the network such that mass conservation, enzyme capacities and thermodynamics is respected. Functional states of the metabolic network, i.e. a particular (mass)flux distribution through the metabolic network, can be identified by a constraint-based convex analysis of the stoichiometric matrix [122], which captures the essential structural features of the metabolic network.

As illustrated above, different modeling paradigms capture biological phenomena at different levels of description. However, they share the unifying concept of (bio)chemical reaction networks (see Figure 2). Chemical reaction networks consist of a set of chemical species (metabolites in the biochemical setting) and a system of reactions that interconvert them. In chemical notation a reaction network is described by a set of chemical equations (see Figure 1 left).

The topology of a chemical reaction network is largely embodied in the stoichiometric matrix (see Figure 1 right). This matrix is organized such that every column corresponds to a reaction and every row corresponds to a chemical species. The entries of the matrix are stoichiometric coefficients, which are positive/negative integers if the chemical species is produced/consumed during the reaction.

The first approaches towards a systematic understanding of chemical reaction networks were based on the analysis of the stoichiometry in mass action-reaction systems [22, 46, 66, 79, 80, 145]. Resulting theorems such as the *zero-deficiency theorem* provide a link between network structure and reaction kinetics [45, 57, 71, 72]. Graph theoretical conditions can be very helpful in guiding the process of model building in systems biology. Depending on the qualitative dynamic behavior (e.g. bistability or oscillation) of the biological system under study, particular network topologies that do not possess the potential to show the desired qualitative dynamics irrespectively of the choice of the kinetic parameters, can be eliminated from the list of potential candidates early on during model development. The `MATLAB` package ERNEST [147], for instance, can be used for model discrimination along these lines.

The zero-deficiency theorem is based on properties of the graph of chemical complexes (see Appendix A for details) and the concept of *weak reversibility*. A reaction mechanism is said to be weakly reversible if for any two complexes in a graph component which are connected by a directed path, there exists a directed path connecting the two complexes in the reverse direction. The deficiency δ of a reaction mechanism can be considered as a measure for the linear independence
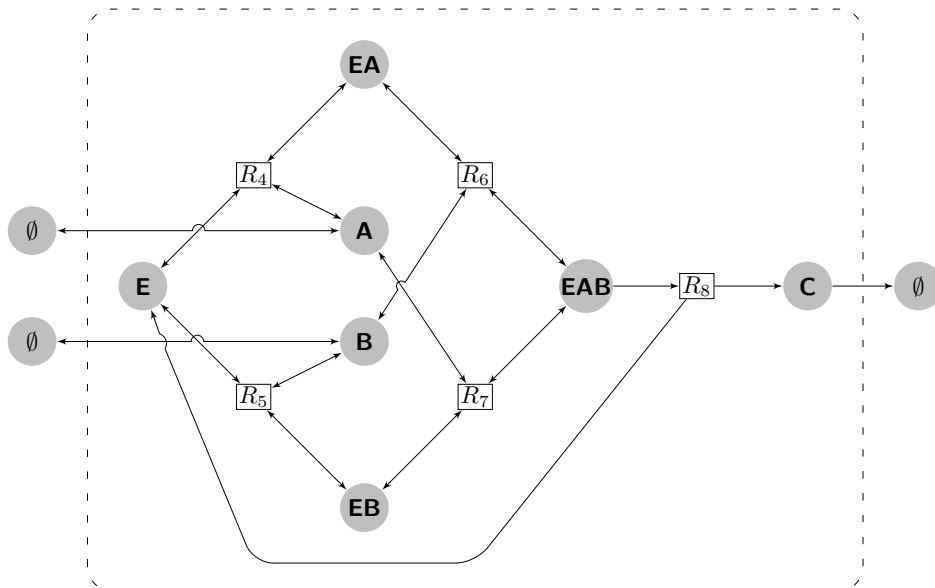
Figure 2. Graph representation of the chemical reaction network from Figure 1. Species nodes are drawn as gray circles and reaction nodes as squares (For clarity the in- and outflow reaction nodes (R_1–R_3) have been omitted). Figures illustrating the major flux modes for this reaction network can be found in Appendix A.

of "necessary" reactions and can be calculated from the reaction vectors building up the stoichiometric matrix. In particular, if a reaction is a linear combination of other reactions in the system, but cannot be eliminated to simplify the reaction mechanism, then the deficiency of the mechanism will be greater than zero.

The zero-deficiency theorem makes two important statements about reaction networks with deficiency $\delta = 0$ that hold for any arbitrary choice of the kinetic constants: (i) If the reaction network is weakly reversible it possesses a single steady state which is asymptotically stable. (ii) If the reaction network is not weakly reversible there exists neither a steady state where all species concentrations are greater zero, nor is there a periodic trajectory in which all species concentrations are positive. In essence the theorem states that only reaction networks with $\delta > 0$ possess the potential to show "interesting" nonlinear dynamics such as oscillations.

Recent work along these lines resulted in further theorems connecting dynamic behavior such as multistability, oscillations [25,111] or the bifurcation structure [112] of mass-action reaction systems to properties of the underlying reaction network. Furthermore graph-theoretical conditions for the detection of Turing bifurcations in mass-action reaction diffusion systems [110] have been found.

It is not straightforward to define the notion of a "metabolic pathway", especially if the metabolic network under consideration is of genome scale. Intuitively a pathway is a subset of reactions that is linked by common metabolites. The problem of partitioning a reaction network into chemically meaningful pathways can be solved by metabolic flux analysis [22, 47, 67, 141]. Here the stoichiometry of the metabolic network is investigated to find direct routes which connect mass flows entering and exiting the metabolic network. A "flux mode" is a set of flux vectors which describes such dominant reaction pathways through the metabolic network [142,144] at steady-state conditions.

$$\frac{d}{dt}x = S \cdot v = \frac{d}{dt} \begin{pmatrix} x_A \\ x_B \\ x_C \\ x_E \\ x_{EA} \\ x_{EB} \\ x_{EAB} \end{pmatrix} = \begin{pmatrix} +1 & 0 & 0 & -1 & 0 & 0 & -1 & 0 \\ 0 & +1 & 0 & 0 & -1 & -1 & 0 & 0 \\ 0 & 0 & -1 & 0 & 0 & 0 & 0 & +1 \\ 0 & 0 & 0 & -1 & -1 & 0 & 0 & +1 \\ 0 & 0 & 0 & +1 & 0 & -1 & 0 & 0 \\ 0 & 0 & 0 & 0 & +1 & 0 & -1 & 0 \\ 0 & 0 & 0 & 0 & 0 & +1 & +1 & -1 \end{pmatrix} \cdot \begin{pmatrix} v_1(x_A, q) \\ v_2(x_B, q) \\ v_3(x_C, q) \\ v_4(x_A, x_E, x_{EA}, q) \\ v_5(x_B, x_E, x_{EB}, q) \\ v_6(x_B, x_{EA}, x_{EAB}, q) \\ v_7(x_A, x_{EB}, x_{EAB}, q) \\ v_8(x_{EAB}, q) \end{pmatrix}$$

Figure 3. The stoichiometric matrix S as linear transformation between the reaction rate vector v and the vector of changes in species concentrations x. In many cases entries in the reaction rate vector v cannot be measured directly and hence must be inferred indirectly from biological data.

From the mathematical point of view the problem is to find the extremal rays of a cone [48, 151] that is determined by the stoichiometric matrix. In particular the (right) null space of the stoichiometric matrix contains the steady-state flux modes through the reaction network. A convex representation of the (right) null space has proven to be chemically and biologically meaningful where the individual extremal rays spanning the convex cone correspond to dominating pathways through the reaction network. Although metabolic flux analysis disregards the kinetics of the reactions nevertheless biologically meaningful states of the reaction network can be predicted which coincide nicely with experiments [74,148]. Many pathogens regulate specific metabolic pathways to optimize their growth conditions inside the host cell. A metabolic flux analysis can pinpoint such essential pathways as potential drug targets.

Metabolic fluxes cannot be measured directly by experimental methods, but must be inferred through model based data evaluation from the knowledge of the involved reactions, the stable isotope labeling patterns in the reporter metabolites (e.g. amino acids) and the imposed external fluxes [134]. Experimentally, glucose with a ^{13}C label at a particular position is provided as food to the micro-organism under consideration. Over time the micro-organism metabolizes the glucose along different metabolic routes and the original ^{13}C label ends up at different positions in the reporter metabolites (i.e. the isotope labeling pattern), depending on which metabolic routes were active. Computationally, often an iterative approach is used that minimizes the mismatch between the predicted isotope labeling pattern generated for a particular choice of the flux distribution through the involved reactions and the experimentally obtained labeling patterns [150]. The minimization of the data mismatch is stopped when it reaches the range of the experimental error. This is an example of the discrepancy principle which will be discussed in section 3.1.5.

A typical feature of metabolic networks, which are among the best characterized networks in systems biology, is the existence of network hubs, i.e. a few nodes which are connected to a large number of other nodes in the network, while most of the nodes in the network possess only a few connections to other nodes. The existence of hubs is directly reflected in the sparsity of the corresponding stoichiometric matrix and is for example one characteristic of *scale-free* networks [8].

Besides the stoichiometric matrix also the vector v of reaction rates, specifying the fluxes through individual reactions, is crucial for the formulation of an ODE model (see Figure 3). Parameters enter the ODE model via v. Parameter values or even the whole functional form of enzymatic rate laws may be inaccessible via experimental measurements or simply unknown, respectively. It has been shown that enzymatic rate laws, which can be highly nonlinear due to allosteric interactions, can differ considerably between *in vivo* and *in vitro* conditions [152]

leading to large discrepancies between the *in vivo* and *in vitro* kinetic characteristics of enzymes. Hence there is a need in systems biology for robust methods making it possible to infer these important parameters from experimental data. The insight gained from simulation results of properly parameterized models may stir the design of further *in vivo* and *in vitro* experiments. The newly gathered data, in turn, boost the development and refinement of the models to bring their description level closer to physical and biological reality.

The efforts in systems biology to build accurate and predictive *in silico* models of biological systems and the rapid development of experimental techniques paved the ground for synthetic biology [4] which seeks, on the one hand, to engineer existing biological systems and, on the other hand, to design *de novo* synthetic networks from well characterized biological parts or non-natural components exhibiting a desired qualitative dynamic behavior.

In analogy to electrical engineering, where complicated functional circuits are built from a handful of well understood and standardized entities such as transistors, resistors etc., efforts are currently under way to compile a similar standardized list of biological objects [16], e.g., the BioBrick registry (`http://partsregistry.org`), a database hosted at MIT's registry of standardized biological parts, is such a collection of genetically encoded functional parts that can be combined to build synthetic biological devices and systems.

The goal of designing and constructing biological devices gives rise, from a mathematical point of view, to multi-level inverse problems: (i) at the bottom level the individual biological entities must be characterized in terms of parameters, (ii) at the next level of assembling the biological device, parameters influencing the coupling of the subsystems must be identified, (iii) finally, putting the biological device into the cellular context will require parameter fine tuning to account for additional interactions between the device and the complex cellular matrix.

2.1. The modeling process in systems biology

The modeling of biochemical systems consists of several steps [21]: (i) collection of experimental data and information on network topology and regulatory interactions, (ii) selection of a level of description and a particular mathematical formalism, (iii) parameter identification and model analysis, and (iv) model validation and refinement.

In step (i), the relevant data are obtained from experiments or data bases and information on network structure and regulation is collected from the literature. Typically, network topology and regulatory interactions are not fully known and hence have to be inferred in the following steps. In step (ii), additional assumptions and simplifications have to be made in order to define the components and interactions of the system which should be included in the mathematical model. A suitable formal framework is chosen – in many cases systems of ODEs – and the symbolic equations are formulated. In step (iii), unknown parameters in the symbolic model are identified, and a numerical model is obtained which is consistent with the experimental data. The mathematical model is analyzed with respect to steady-states, stability, parameter sensitivities, and bifurcations. In step (iv), the model is tested with data which have not been used for model construction. Additionally, all assumptions made in the previous steps are reconsidered and refined, since modeling is a cyclic rather than a linear process. Upon completion of the modeling process, predictions can be made, new hypotheses can be generated, new experiments can be designed, and the biological system can be optimized.

ODE model types prevalent in systems biology

In biochemical systems, the underlying processes are of a stochastic and spatial nature and can take place at different time scales. For simplicity, ODE models are frequently used to approximate these processes, but the validity of such approximations has to be checked on an individual basis. For example, ODE models may be appropriate for systems where diffusion and transport processes are fast compared with chemical reactions and where molecular species are present in high numbers. In order to state a general ODE model, assume there are n molecular species present in quantities $x \in \mathbb{R}^n$, and let there be l interactions occurring at rates $v(x) \in \mathbb{R}^l$. Typically, the rate laws also depend on parameters such as kinetic constants, equilibrium constants, so-called Hill coefficients, and other (known or unknown) empirical quantities. Hence, we replace $v(x)$ by $v(x, q)$ thereby introducing m parameters $q \in \mathbb{R}^m$. Now, the time evolution of the system can be written as

$$\frac{dx}{dt} = f(v(x, q)). \tag{1}$$

The function $f : \mathbb{R}^l \to \mathbb{R}^n$ combines the contributions of the individual interactions to the production or consumption of the individual species.

Mathematical models of *metabolic networks* capture both the stoichiometry and the kinetics of chemical reactions. The stoichiometry of a pathway system determines its topology and is represented by the stoichiometric matrix S. For metabolic networks, eqn. (1) takes the form

$$\frac{dx}{dt} = Sv(x, q). \tag{2}$$

In this case, the function f is simply the stoichiometric matrix S and hence linear. This assumption of linearity is also common beyond pathway systems, e.g. in models of gene regulatory networks, see below. The generic nonlinearity of biochemical systems is hidden in the rates $v(x, q)$, which are determined by the kinetics of the reactions.

Specific forms of the rate laws in eqn. (2) are used based on assumptions on the underlying kinetics. The most common choices are: (i) mass-action kinetics, (ii) Michaelis-Menten kinetics, and (iii) ad-hoc approaches such as convenience kinetics. Models based on the law of mass action are typically used to describe networks of elementary reactions. The rate of the jth reaction is given by

$$v_j = k_j \prod_{i=1}^{n} x_i^{g_{ji}}, \quad j = 1, \ldots, l, \tag{3}$$

where $k_j \in \mathbb{R}^+$ is the rate constant and $g_{ji} \in \mathbb{N}_0$, $i = 1, \ldots, n$, are the kinetic orders which correspond to the numbers of molecules consumed by this reaction. Mass-action models can be derived from basic principles, however, most biochemical reactions are catalyzed by enzymes and consist of several (possibly many) elementary steps, some of which may even be unknown. Hence, for large pathway systems it is advisable to use composite rate laws for enzymatic reactions [24], and the most widely-used representative of this category is Michaelis-Menten kinetics. This approach is based on the concept that substrate and enzyme form one or more intermediate complexes before the product is released and the enzyme is regenerated. Furthermore, it is *assumed* that concentrations of the intermediate complexes are approximately constant over time (quasi-steady-state-assumption). For basic enzyme mechanisms, the resulting rate laws are simple: for example, let

the jth reaction follow the irreversible Michaelis-Menten mechanism [24]; then the corresponding rate law amounts to

$$v_j = V_j \frac{x_i}{K_j^M + x_i}, \qquad (4)$$

where V_j is the limiting rate, K_j^M the Michaelis constant, and x_i the concentration of the substrate converted by the reaction. For complex mechanisms, however, the Michaelis-Menten rate laws contain many parameters which are difficult to interpret in terms of the function of the enzyme and difficult to infer from experimental data. In these cases, ad-hoc approaches come into play. Convenience kinetics, for example, covers enzyme regulation by activators and inhibitors and can be derived from a random-order enzyme mechanism. In order to ensure thermodynamic correctness, rate laws are written in terms of thermodynamically independent parameters, such as particular equilibrium constants, mean turnover rates, generalized Michaelis constants, and parameters for activation and inhibition, see [101].

Using customized rate-laws for each (enzymatic) reaction can sometimes hide the pattern of regulation (activation and inhibition), in particular in large pathway systems. A good compromise that is capable of capturing the regulatory interactions in a metabolic network while keeping the mathematical description relatively simple is the use of so-called canonical models which have a pre-defined structure and which differ only in their parameter values [21]. Due to their homogeneous structure, canonical models are easily scalable and allow the development of specialized techniques for symbolic and numerical analyses. The most prominent representatives of canonical models are S-systems [135–137]. In these models, production and consumption are approximated by products of power-law functions. The ODE of the ith molecular species has the following form:

$$\frac{dx_i}{dt} = \alpha_i \prod_{j=1}^{n} x_j^{g_{ij}} - \beta_i \prod_{j=1}^{n} x_j^{h_{ij}}, \quad i = 1, \ldots, n, \qquad (5)$$

where $\alpha_i, \beta_i \in \mathbb{R}^+$ are rate constants and $g_{ij}, h_{ij} \in \mathbb{R}$ (usually $\in [-1, +2]$) are kinetic orders quantifying the effect that the jth species has on the production or consumption of the ith species. A positive, negative, or zero kinetic order corresponds to an activating, inhibitory, or no effect, respectively. Canonical models have a number of advantageous features. They are characterized by a correspondence between structural features and parameters. The models can be set-up without knowledge of the underlying regulatory network, but if structural features are known, then it is obvious which parameters in the model are affected, and vice versa, if a parameter has been identified, then its interpretation in terms of a structural feature is clear. For S-systems, steady-states can be computed symbolically and specialized numerical methods have been proposed to identify parameters [20].

The previous paragraphs reviewed ODE modeling approaches for metabolic networks. Now, we turn our attention to *gene regulatory networks*. Besides a variety of other formalisms (such as graphs, Boolean networks, Bayesian networks, and generalized logical networks, cf. [29]) ODE systems are widely used to analyze gene regulatory networks. The fundamental processes of regulator binding, transcription, translation, and degradation can be modeled at various levels of detail. Traditionally, ODEs are formulated for mRNAs and proteins; other molecular species such as polymerases, nucleotides, ribosomes, and amino acids are supposed to abound, and hence their concentrations need not enter the models. Assume there are n genes, and let the mRNA and protein concentrations be x_i^{m}

and x_i^{p}, $i = 1, \ldots, n$. Then, the corresponding ODEs have the form

$$\frac{dx_i^{\mathrm{m}}}{dt} = k_i^{\mathrm{ts}} f_i(x_1^{\mathrm{p}}, \ldots, x_n^{\mathrm{p}}) - d_i^{\mathrm{m}} x_i^{\mathrm{m}}, \tag{6a}$$

$$\frac{dx_i^{\mathrm{p}}}{dt} = k_i^{\mathrm{tl}} x_i^{\mathrm{m}} - d_i^{\mathrm{p}} x_i^{\mathrm{p}}, \tag{6b}$$

where k_i^{ts}, k_i^{tl} are transcription and translation constants, respectively, and d_i^{m}, d_i^{p} are degradation constants. The nonlinearity is hidden in the regulation functions $f_i(x_1^{\mathrm{p}}, \ldots, x_n^{\mathrm{p}})$, which determine how one gene is activated or inhibited by the other genes.

The most common regulation functions are: (i) customized functions, (ii) sigmoid functions, and (iii) step functions [29]. In principle, regulator binding can be modeled using mass-action kinetics and the quasi-steady-state-assumption for the gene-regulator complexes, see above. The knowledge of both binding kinetics and regulation logic allows the derivation of a customized function, which determines the activation or inhibition of one gene by the other genes [115,160]. However, many genes have several regulatory sites (such as in the case of cooperative binding) and the resulting regulation functions may become very complicated. In these cases, it is common to use sigmoid functions to model the typical switching behavior in gene regulation. For example, let the ith gene be activated by the jth protein in cooperative manner. Then, the regulation function is usually approximated by

$$f_i(x_j^{\mathrm{p}}) = \sigma^+(x_j^{\mathrm{p}}, K_i, n_i) = \frac{(x_j^{\mathrm{p}})^{n_i}}{(x_j^{\mathrm{p}})^{n_i} + (K_i)^{n_i}}, \tag{7}$$

where K_i is the concentration of half-activation (determining the threshold of the switch) and n_i is the Hill coefficient (determining the steepness of the switch). This formula can be regarded as purely empirical and the Hill coefficient need not be integer. A further simplification can be made by replacing the continuous sigmoid functions by discontinuous step functions (corresponding to the limit $n_i \to \infty$). This assumption turns (6) into a system of piecewise-linear ODEs, more specifically, the state space becomes divided into n-dimensional hypercubes in which the regulation function is constant and degradation is linear. Each hyper-cube corresponds to a qualitative state of the system, and the qualitative dynamics of the system can be represented by a transition graph [50]. As a consequence, methods from qualitative reasoning become applicable, in particular a formalism called qualitative differential equations [90, 91].

In case the regulation logic of a gene network is not known or the precise mechanisms are inaccessible, S-systems can be used as base models for gene regulatory networks. Due to their pre-defined structure, S-systems are also well suited for comparing the functional effectiveness of different types of gene regulatory networks [138, 139].

2.2. Parameter identification in systems biology

A challenging task in the mathematical modeling of biochemical systems is the identification of parameter values. As stated above, parameter identification is connected with other tasks such as the inference of network topology, the definition of system components and interactions, and the choice of a mathematical formalism. Clearly, size and complexity of the resulting model affect the difficulty of parameter identification (and later analyses).

From a historical point of view, the quantity and quality of available experimental data has determined the application and development of mathematical methods

for parameter identification in systems biology. As an example, we consider the case of metabolic networks: traditionally, biochemists studied individual enzymes *in vitro*; they identified co-factors and effectors and measured initial rates for different substrate and effector concentrations; with this data, they parameterized mathematical models such as the Michaelis-Menten rate law by using linear regression. Once models had been derived for the individual enzymatic processes, this information could be merged into an integrative pathway model in a so-called *bottom-up* strategy [21]. The major disadvantage of this strategy is that information about individual enzymes is derived from diverse sources, i.e. experiments conducted under different conditions or even for different organisms. Hence, many times the integration of individual models is not successful and requires model refinement and additional experimental data. Recent advances in technology allow for a completely different approach to parameter identification using a so-called *top-down* strategy. Modern high-throughput techniques provide time-series measurements of genes, proteins, or metabolites on a cellular or even organismal level. Ideally, the data are generated *in-vivo* and with minimal disturbance of the biological system. This comprehensive data at the system level can be used to infer parameters at the component level. However, the information on model parameters contained in time-series measurements is only implicit and has to be extracted by using suitable mathematical methods. This important inverse problem is one main focus of this review.

Amongst the parameter identification methods traditionally used in systems biology, the predominant strategy consists of finding parameter values that minimize the data mismatch, i.e. the discrepancy between the experimental observations and the simulated data. The underlying premise is that the optimal parameter set is one which gives rise to simulated data that match the experimental observations as well as possible. Computationally, the minimization of the objective function may involve a combination of local (gradient-based) and global (mostly stochastic) methods [113,126]. Since for certain parameters even the order of magnitude may be unknown, it is important to complement the rapid convergence of local optimization algorithms with the comprehensive nature of global search techniques.

Due to the difficulty of in-vivo measurements and the complexity of cellular environments, data error is inevitable in the time-series measurements of biochemical species. Faced with the noise present in biological data, one naturally asks the question: how does the inaccuracy in the measurements propagate back to errors in the inferred parameters [58, 76, 88, 127]? Many mathematical models of biochemical networks exhibit a wide spectrum of parameter sensitivities with eigenvalues distributed over several orders of magnitude [61]. This indicates the *ill-posedness* of the parameter identification problem, in particular the instability with respect to data noise. Ill-posed inverse problems have long been studied in the mathematical literature, and *regularization techniques* have been developed which control the impact of the data error, cf. [38]. For systems consisting of many components, this issue becomes especially important since the instability of the identification problem typically grows with the number of unknown parameters. Thus, the development of strategies for identifying parameters in a reliable manner is an important mathematical problem with significant practical implications [95]. In Section 3.1, we present regularization techniques and demonstrate their significance for systems biology by examining a benchmark problem that has been widely studied in the noise-free case [78,113,126,164]. By adding noise to simulated data, we show that such a benchmark parameter identification problem is in fact highly unstable. Moreover, we demonstrate that Tikhonov regularization can be effectively used to identify parameters in a stable way even in the presence of data noise.

Finally, we address the inference of network topology which ideally precedes the process of parameter identification. Whenever some interactions between system components are unknown, even the formulation of the mathematical model becomes unclear. Mathematical techniques for structure identification can be divided into two groups. First, model-free methods depend only on the data. For example, one can infer the Jacobian matrix of a system from transient responses to small perturbations of a steady state [18] or read off the topological distances of the network components from temporal responses to perturbations of arbitrary size [157]. In another approach, time-lagged correlations between system components are calculated from responses to large-amplitude noise. Using correlation metric construction (CMC), the topology of the network as well as the strength of the interactions can be reconstructed [5].

The second group consists of model-based methods. As stated above, it is not clear a-priori which mathematical model is appropriate to account for unknown interactions between system components. Additionally, the introduction of hypothetical interactions may result in a combinatorial explosion of the number of parameters, which in turn may cause the problem of over-fitting of the experimental data. On the other hand, biochemical networks are typically sparse, i.e. genes, proteins, or metabolites interact with only few other genes, proteins, or metabolites. In fact, most biochemical species take part in less than four or five processes each [77, 109]. Hence, one may add to the data mismatch a penalty term discriminating against parameters which have only little effect on the system dynamics. First studies were done for S-systems, which are characterized by a one-to-one correspondence between network interactions (activation or inhibition of production or consumption processes) and parameters (kinetic orders). In this case, network inference becomes a parameter identification task. As a penalty term, the sum over the absolute values of unknown kinetic orders [85] (l_1-norm) or the number of non-zero parameters [49] (l_0-"norm") have been used. The latter approach has the disadvantage that it turns the minimization of the objective function into a combinatorial problem. The use of different norms in the penalty term has been intensively studied in the mathematical literature [28, 104, 123, 163]. In particular, it has been shown that the problematic l_0-"norm" mentioned above can be approximated by the l_p-quasinorm with $0 < p < 1$, which additionally has a stabilizing effect on the ill-posed problem of parameter identification. Hence, this approach is referred to as *sparsity promoting regularization*.

2.3. Qualitative Inverse Problems

2.3.1. Bifurcation analysis in cellular physiology In the modeling of genetic and metabolic networks, from quantitative data and database knowledge, ODE models of the form (1) are derived; refer to Appendix C for an example. With the parameter values q corresponding to the given physiological conditions and input signals, the time-course trajectory can be computed. In building models in biology, often the desired quantitative data or even the knowledge of the network topology may be incomplete. Hence, at the initial modeling stage one might ask the following question: given the current state of knowledge in molecular biology as has been captured in the mathematical model, can it be consistent with the known *qualitative* features of the cell physiology? Such observed features might be the presence of geometric patterning or the multi-stability of the cell state as reflected in its path dependence [44]. After exploring a given model of a network for the range of parameters that lead to qualitative dynamics consistent with that of the biological system under consideration, parameter identification from time-course data could be carried out, starting within the range thus obtained. While the particular
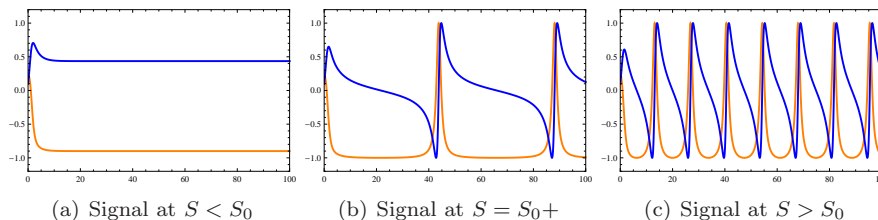
(a) Signal at $S < S_0$ (b) Signal at $S = S_0+$ (c) Signal at $S > S_0$

Figure 4. Transition across a Saddle-Node Invariant Cycle (SNIC) bifurcation as S varies: time courses

form of the system trajectory may determine the quantitative details of cellular responses, there often exists a more direct relation between the cell physiology with the qualitative dynamics of the ODE system as captured in the *bifurcation diagrams* [54, 155]. In particular, at most parameter values as the parameters q vary in a small neighbourhood, the qualitative behavior of the dynamical system remains the same. At bifurcation points, the dynamical system loses its structural stability: for instance, additional equilibria may emerge (as in the case of the *saddle-node bifurcation*) or oscillations may appear from a stable equilibrium point as the systems crosses a *Hopf bifurcation* [92].

In the context of cell physiology, bifurcations correspond to the presence of thresholds across which the cell responds in qualitatively different ways with respect to the input signal. In particular, the presence of bifurcations in systems biology networks (including genetic, signal transduction, neuronal and developmental networks) have important implications for its associated information-processing functions [75, 154, 155]. For instance, in the context of signal transduction networks, the bifurcation parameter would be the level of the ligand (or triggering) molecule, and the *system parameters* would be kinetic constants that would determine the type of dynamic response that is triggered; different tasks of direct and inverse types arise in studying these problems.

We now illustrate via an example the link from bifurcation diagrams to the cell physiology. Let us consider a sub-module of a regulatory system which exhibits the following qualitative behavior: under a sufficiently low range of input signal, S, the system exhibits a stable steady-state behavior, giving rise to a certain protein concentration level that increases with the signal size; however, as the input signal size crosses a threshold S_0, long period oscillations begin to appear. As the signal increases even higher, oscillations occur at an increasingly higher frequency; Figure 4 depicts this behavior. Given this qualitative information, one might ask if it could be captured in a ODE model. In Figure 5 we show a sequence of phase portrait where this dynamics would be realized: plot (a) shows that for low values of the signal strength the system has a single stable steady-state (denoted as the filled circle), which in (b) coalesces with an unstable state state as the signal increases towards the threshold S_0 and subsequently disappears, leaving a limit cycle solution shown in (c). The depicted scenario is the *Saddle-Node on Invariant Circle* (SNIC) bifurcation [92]; the limit cycle solution that appears subsequent to the SNIC bifurcation has a long period; in fact the period scales asymptotically as $\sim \frac{1}{\sqrt{S-S_0}}$ due to the effect of the "shadow" that remains in the vector field following the disappearance of the saddle-node [92] (see the shaded region in Figure 5(b)). Therefore, in modeling a system that has the above described phenomenon, one might wish to find molecular interactions that could give rise to the bifurcation diagram shown in Figure 6; we call problems of this type *qualitative inverse problems*, since the aim is to determine parameter configurations that give rise to a specified qualitative behavior.
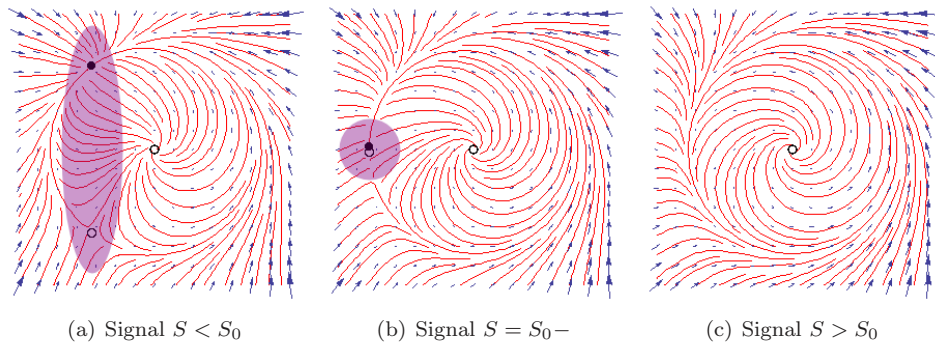
(a) Signal $S < S_0$ (b) Signal $S = S_0-$ (c) Signal $S > S_0$

Figure 5. Transition across a Saddle-Node Invariant Cycle (SNIC) bifurcation as S varies: phase portraits
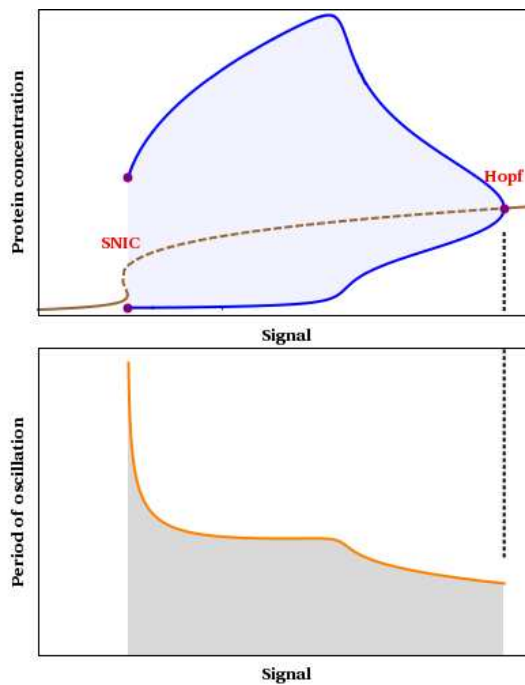

Figure 6. Bifurcation diagram of a system undergoing Hopf and SNIC bifurcations. **Top figure**: at low values of the signal, there exists a stable steady state (solid line) which subsequently loses stability via the SNIC bifurcation (the curve of unstable equilibrium is shown as a dashed line); further along the curve, the equilibrum undergoes a Hopf bifurcation, from which a stable limit cycle solution comes off (the curve of minima and maxima of limit cycle is denoted by the solid blue lines). **Bottom figure**: the period of oscillation for the limit cycle solution shows a blow-up $\sim \frac{1}{\sqrt{S-S_0}}$ near the SNIC bifurcation.
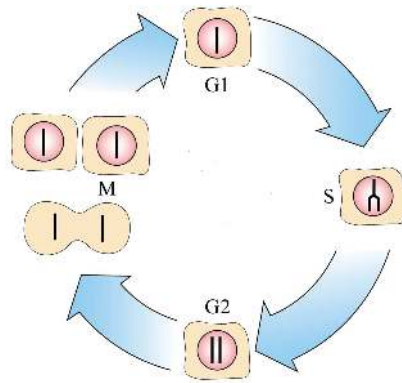
Figure 7. The cell division cycle: In the Gap 1 (G1) phase cells grow in size, preparing for the Synthesis (S) phase during which DNA duplication occurs; in the Gap 2 (G2) phase cells continue to grow until Mitosis (M) phase is reached and the cells divide.

In dynamical processes observed in biology, the time-course trajectory can often be divided into phases of different qualitative behaviors. For instance, in models of the cell division cycle [155], as the mass of the cell increases, the system transitions (via a SNIC bifurcation) from one having a bistable state to one with a limit cycle attractor. Such bifurcation diagrams containing various arrangements of saddle-node, Hopf and SNIC bifurcations as in Figure 6 can be observed in models of gene networks containing coupled negative and positive feedback *regulatory motifs* [120, 156]. The regulatory function of the gene network can, in turn, be understood by reading off the bifurcation structure. For instance, for a periodic regulator which has the bifurcation diagram shown Figure 6, the decrease in the oscillation period away from the SNIC bifurcation could go towards compensating a variable rate of signal growth; such a feedback mechanism goes towards ensuring the balanced growth and division that is of crucial importance in *cell cycle* models [26, 155] that describe the sequence of events that leads to the division and replication of cells; refer to Figure 7 for the sequence of events that occur from the Gap 1 (G_1), to Synthesis (S), Gap 2 (G_2) and Mitosis (M). As an illustration of the role of gene networks controlling the cellular state, we look at the bifurcation diagram shown in Figure 8, of a bistable switch model governing the G_1/S transition in mammalian cell cycle [149]; the full ODE model is given in Appendix C. The solid lines in Figure 8 correspond to different physiological states: the G_1 and the S phases. The transitions between the phases correspond to transcritical (TC) and saddle-node (SN) bifurcations in the model. Different physiological conditions may lead to shifts in the parameters in the regulatory system and may change the bifurcation diagram. For instance, the triggering of a *check-point* mechanism [155] would lead to a delay in the switching point to a higher level of the input signal; see the top diagram in the right of Figure 9.

We remark that saddle-node and Hopf bifurcations are examples of co-dimension 1 bifurcations [92]; there are bifurcations of co-dimension 2 and higher, which act as *organizing centers* around which the various one-parameter bifurcation diagrams are possible. Shown in Figure 10 is an illustration of a cusp singularity, showing that lines of saddle-node (or fold) singularities emerge from it.

So far, we have looked at example systems where the gene regulatory system responds to a given input signal and the associated bifurcations of equilibria have physiological significance in terms of transitioning between the states of the cell. An important class of phenomena prevalent in biology is the presence of oscillatory
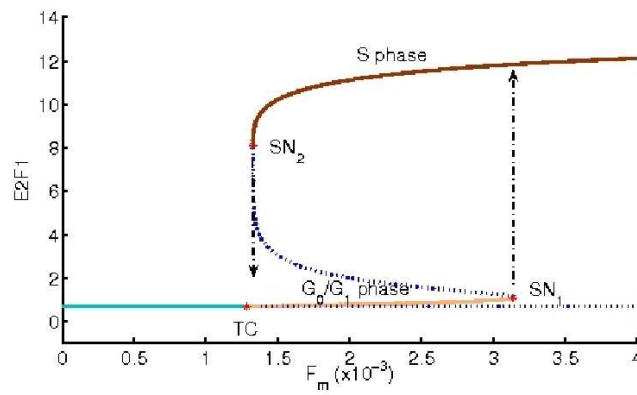
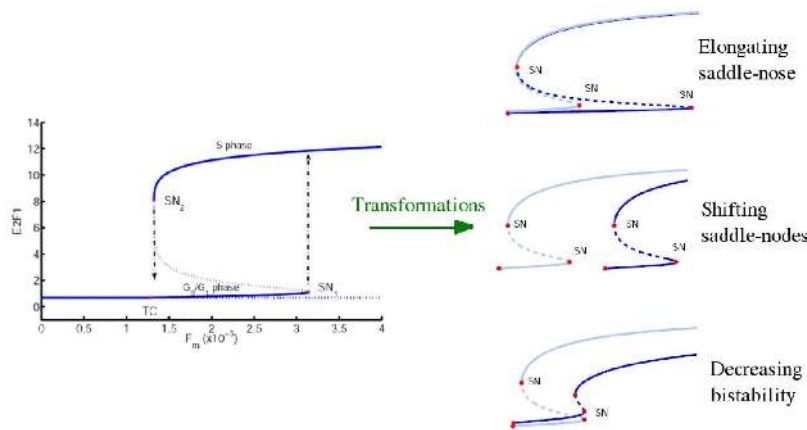**Figure 8.** Bifurcation diagram of a model underlying G_1/S transition [149]

Figure 9. Possible transformations of bifurcation diagram for a bistable switch
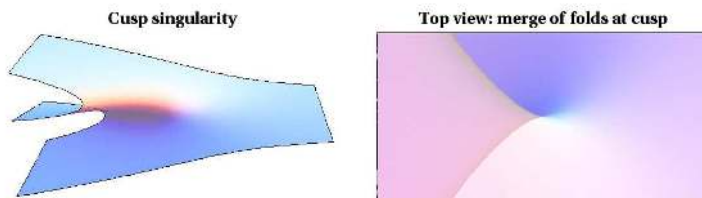

Figure 10. Cusp singularity and fold curves that come off it

phenomena occurring at multiple time-scales. These dynamical phenomena could be understood either via the bifurcation diagram in the interplay between fast and slow variables, or arise as bifurcations of limit cycles. For instance, Figure 11 shows bursting dynamics commonly observed in some cell types, including neurons and endocrine cells [44,75]. Bursting dynamics as shown in Figure 11 can be dissected as an alternation between two disparate time-scales: the fast, spiking phase in between the slow, recovery phase. The trajectory of the combined fast-slow variables and the nullclines of the fast subsystem are represented in Figure 12(a). As the slow variable
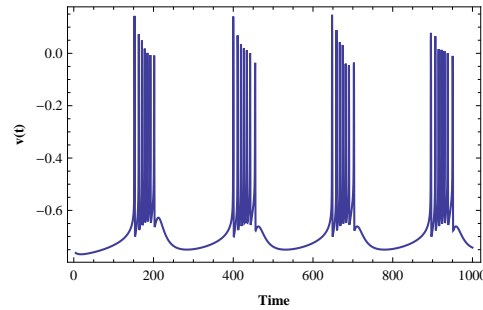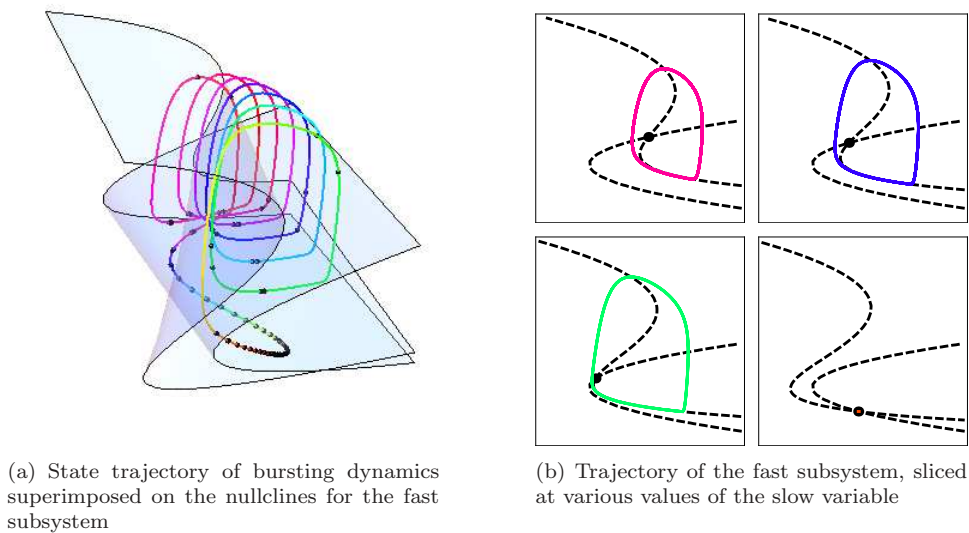
Figure 11. Bursting dynamics: an interplay of fast and slow time scales

(a) State trajectory of bursting dynamics superimposed on the nullclines for the fast subsystem

(b) Trajectory of the fast subsystem, sliced at various values of the slow variable

Figure 12. Trajectory of system and phase portraits

changes, the fast sub-system is taken through the sequence of phase portraits shown in Figure 12(b), which undergo bifurcations at the start and end of each spiking phase. Therefore, by studying the bifurcation diagram of the fast subsystem one can gain an understanding into the roles the underlying physiological mechanisms giving rise to the bursting behavior.

Oscillations are prevalent in biology, the most prominent of which is that of the circadian rhythm clock [97], whose free-running period is close to 24 hours and plays an important role in the orchestration of various biological processes. However, in addition to the circadian rhythm, there are periodic processes occurring at significantly smaller or larger time scales. For instance, metabolic oscillations with periods of around 40 minutes have been observed in yeast, in which cells undergo reductive and oxidative phases [86] and dynamic effects such as modulated oscillations or period-doubling bifurcation have been observed in metabolic data [100]. The periodic arousal events observed in hibernating arctic squirrels provide an example of regular oscillations occuring at a time scale significantly longer than a day [161, 162]. In particular, Figure 1 of [161] shows arousal events which appear regularly, with a period of approximately 20 days; it is hypothesized that these arousal episodes are necessary to avoid brain damage in the arctic squirrel. While
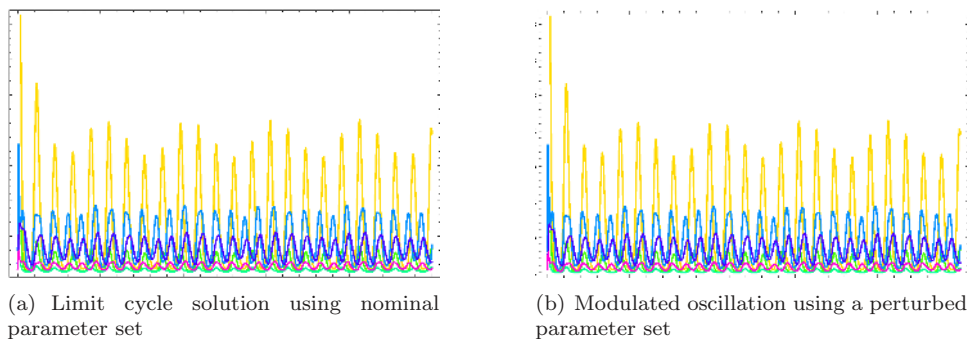
(a) Limit cycle solution using nominal parameter set

(b) Modulated oscillation using a perturbed parameter set

Figure 13. Time-course of the 3-loop circadian rhythm system proposed in [102]
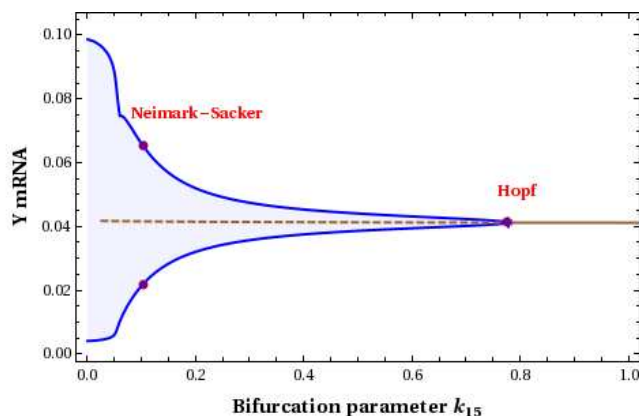

Figure 14. Bifurcation diagram of the 3-loop circadian rhythm system proposed in [102]

it has been observed that a peak in the activity of circadian rhythm genes appears early in the arousal events [161], it remains unclear which molecular mechanisms underlie such periodic arousal events. Methods as described in Section 3.2 might be helpful in addressing such questions. Whether and how different rhythms may influence one another across time scales is a question that remains to be addressed.

As an illustration of the possibility for a system to exhibit oscillations at multiple time scales, we look at a circadian rhythm model for *Arabidopsis* [102]. Shown in Figure 13(a) is the limit cycle oscillations obtained for nominal parameter values. By choosing parameters such that the system undergoes the *Neimark-Sacker* bifurcation of limit cycles, the behavior shown in Figure 13(b) is obtained, showing modulated oscillations whereby a slower, oscillatory envelope appears. A bifurcation diagram of the system is shown in Figure 14, showing that the limit cycle solution undergoes such a bifurcation [92]. Subsequent to this bifurcation, the trajectory of the system changes from having a loop-like trajectory (Figure 15(a)) into one that traces out a torus structure (Figure 15(b)).

2.3.2. *From bifurcation phenotype to mechanisms* Given the above described examples illustrating the role of qualitative dynamics in governing cell phenotypes, many qualitative inverse problems arise. In contrast to the standard forward bifurcation analysis which maps molecular interactions to physiological
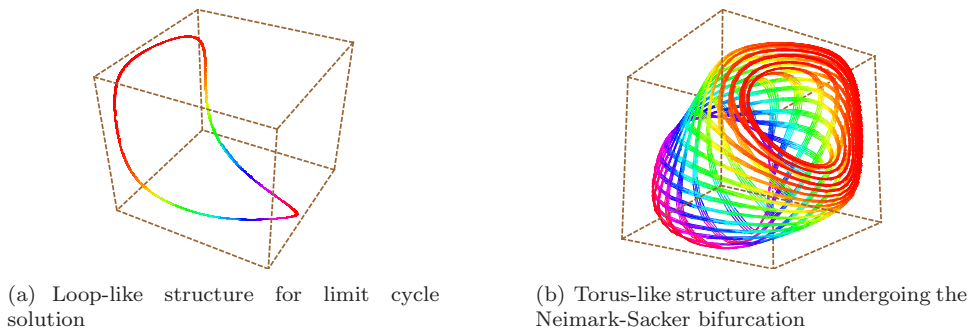
(a) Loop-like structure for limit cycle solution

(b) Torus-like structure after undergoing the Neimark-Sacker bifurcation

Figure 15. State-trajectories of the 3-loop circadian rhythm system proposed in [102]

consequences, *inverse bifurcation* analysis aims to map desired or observed phenotypic characteristics to molecular interactions [104, 105]; applications of such inverse problems range from reverse-engineering the dynamics of gene networks, the design of qualitative behavior for therapeutic treatments (for instance, correcting *dynamics diseases*) or synthetic biology (for instance, a bistable switch out of BioBrick [146] components). In many of these applications, the sparsity of solution is of practical importance, since it allows for obtaining the desired goal with as few changes in the parameters as possible.

Reverse-engineering of gene networks An important question that arises in the modeling of circadian clocks in organisms such as *Drosophila*, is figuring out the reasons for the robustness of oscillation period against variations to poorly controlled parameters (such as degradation rates) or environmental conditions such as temperature. Physiologically, this dynamical property is important in order to ensure that the proper ordering of biological processes that occur throughout the day in spite of changing environmental conditions [96, 98]. To address such questions, computational analyses can be a useful tool in characterizing dynamical properties of circadian clocks and how they arise from the system architecture [124, 125]; see also an numerical example in Section 3.2.3 examining robustness with respect to a specific parameter. On the topic of what are the causes of temperature compensation, a number of competing hypotheses have been proposed, for instance through balanced control coefficients [131] or a resetting mechanism as in many of the previously proposed cell cycle models [70]. In an effort to help answer these inverse problems computational optimization was used to examine possible ways of tuning model parameters to obtain a temperature-compensated model [1, 132].

Diseases and therapeutic treatments As we have shown in the previous examples, the presence of certain bifurcations and/or the geometric relations between bifurcation points may be needed for the correct physiological functioning. Via genetic mutations or other factors, changes may be brought to gene regulatory networks such that they no longer function normally. This could lead to a *dynamical disease*, which was coined by Glass and Mackey [51] as one *that occurs in an intact physiological control system operating in a range of control parameters that leads to abnormal dynamics and human pathology*. For instance, in the context of circadian rhythm, dysfunctions can lead to a number of physiological disorders such as Familian Advanced Sleep Phase Syndrome (FASPS), Delayed Sleep Phase Syndrome (DSPS) [99]. Finding the combination of factors that causes a dysfunctional

bifurcation diagram is an application of inverse qualitative analysis [104].

Synthetic biology Synthetic biology is an emerging field with the goal of developing engineering-like approaches for piecing together molecular components so as to carry out certain pre-defined functions, in much the same spirit as electrical circuits are built from elements such as capacitors and resistors. For instance, one could study the question of how to design a robust circadian oscillator, from the catalogue of parts available in BioBrick [146]. Such design problems give rise to the mathematical and computational challenges of not only the forward but also of the inverse type [36]. Given the physiological implications of qualitative dynamical characteristics, in the design problems arising in biotechnology and pharmaceutical contexts it is of much interest to infer mechanisms that could alter bifurcation diagrams of gene networks [17, 36]. The long-term applications of inverse qualitative techniques could include controlling the differentiation points of stem cells or the construction of robust synthetic switches that are activated by the presence of certain chemicals [17, 83].

In all the application areas mentioned above, there would most likely exist many solutions to the stated inverse problem. However, within the complex networks encountered in biology, one typically wishes to look for the simplest mechanisms, or tunable 'knobs', underlying the observed or desired dynamical effects. This leads us to consider the use of sparsity-promoting regularization in our work: by attributing the data or effects to a few genes or specific interactions, the identified solution would have the advantage of being much more useful within the biological setting [27, 104] or easier to implement as a design task.

3. Methodology

3.1. Parameter identification

3.1.1. Problem Formulation and Ill-Posedness As mentioned above, parameter identification is an essential modeling step in the field of systems biology and is frequently addressed in the respective literature and both in commercial and freely available systems biology toolboxes. Most of the techniques used there are driven by the underlying premise that the optimal parameter solution is one which closes the gap between numerical simulations and experimental observations as much as possible. However, in doing so, the ill-posedness inherent to parameter identification and well studied in the mathematical literature on regularization of nonlinear inverse problems is ignored such that large error propagations from the data to the solution have to be expected. In biological applications, where the data error is especially large and may in fact dominate over the data, error amplification may have severe consequences in terms of way-off parameter estimates. This effect, which is stronger the higher the number of unknown parameters is, makes the use of regularization methods necessary in order to obtain stable results. In this section we present some standard techniques as well as recent results on sparsity enforcing regularization that were partially motivated by our work in systems biology.

In order to illustrate the above mentioned effects of ill-posedness in context of parameter identification in systems biology we consider the metabolic pathway model described in Appendix B. The inverse problem studied is to identify the 36 model parameters from time courses of the 8 species concentrations involved, observed at various time instants under 16 different experimental conditions. In fact, this task has become a benchmark problem for testing parameter identification tools for systems biology, however, mostly for the purpose of comparing the
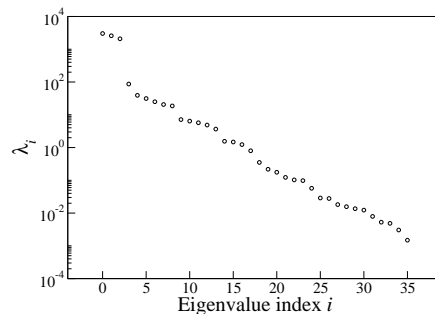
Figure 16. Exponential decay of the eigenvalues of the matrix $F'(q_*)^*F'(q_*)$, indicating the severe instability of the inverse problem. (Note the logarithmic scaling.)

computational efficiency of algorithms, [113]. If we denote by q the parameter vector to be determined and by y^δ the available noisy data (later on δ will play the role of a bound on the data noise), then the inverse problem can be formulated as a system

$$F(q) = y^\delta \tag{8}$$

of nonlinear equations. Here, $F = G \circ S$ represents the so-called parameter-to-output map that is defined as the concatenation of the ODE solution operator S that maps a given parameter vector q (out of a set of admissible parameters Q) onto the solution vector x of the underlying ODE system (1) (where different ODE systems arise in case of different experimental settings) and the observation operator G that evaluates x at those time points the experimental observations are taken.

As solvability of (8) in the strict sense cannot be expected due to data errors and model imperfections, the system (8) is frequently replaced by a nonlinear least squares problem. In our operator formalism the above mentioned pursuit of the "optimal" parameter solution then amounts to solving the minimization problem

$$\|y^\delta - F(q)\|_Y^2 \to \min_{q \in Q}, \tag{9}$$

where $\| \cdot \|_Y$ is an appropriate norm for measuring the discrepancy between data and simulated output. In our example, the noisy data was generated by numerical integration of the ODE system given in Table 1(a) of Appendix B using the initial values given in Table 1(b), the "true" parameter values q_* given in Table 1(c) and the experimental settings given in Table 1(d). Subsequently, this "exact" data $y \equiv F(q_*)$ was perturbed such that the resulting relative error of y^δ was 1%. The bound for the local absolute condition number of the first order necessary condition

$$F'(q)^*(y^\delta - F(q)) = 0 \tag{10}$$

for a minimizer of (9) is proportional to $\lambda_{max}/\lambda_{min}$, where λ_{max} and λ_{min} denote the largest and smallest eigenvalue of the matrix

$$F'(q_*)^*F'(q_*). \tag{11}$$

In the example considered we have $\lambda_{max}/\lambda_{min} \approx 10^6$ and hence expect an ill-conditioned problem. The high data instability of the problem is also underlined by the exponential decay of the eigenvalues of $F'(q_*)^*F'(q_*)$ shown in Figure 16, from which strong error amplifications of noise components over a wide range of frequencies have to be expected.
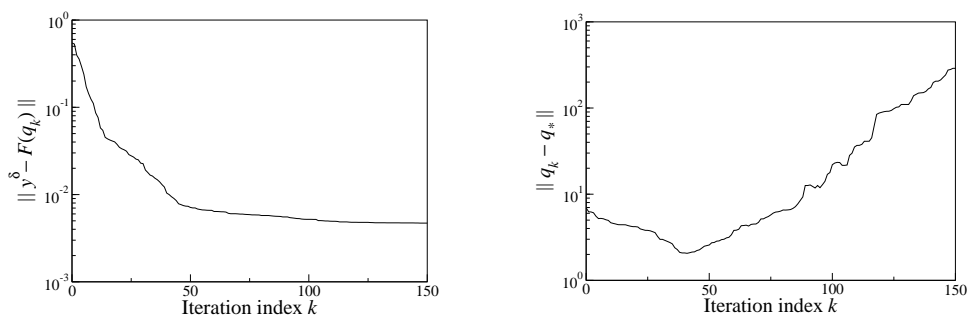
Figure 17. Typical behavior of an iterative method if applied to an ill-posed problem $F(q) = y^\delta$ with noisy data. While the output error $\|y^\delta - F(q_k)\|$ drops monotonically, the solution error $\|q_k - q_*\|$ starts to increase after an initial decrease due to data error propagation. Hence, in order to yield a reliable solution, the iteration has to be stopped at the right time.

This error amplification is illustrated in Figure 17 where the course of an iterative minimization of the least squares functional in (9) is plotted. While the residual norm $\|y^\delta - F(q_k)\|_Y$ monotonically drops as the iteration number k increases, the error $\|q_k - q_*\|_Q$ between the iterate q_k and the true parameter q_* shows the semi-convergence behavior that is typical for ill-posed problems: though the error initially decreases, after some iteration steps the data noise propagation prevails and causes the parameter iterate q_k to diverge from the true solution q_*. This clearly shows the danger that comes along with the approach (9) to solve the parameter identification problem. With the output residual $\|y^\delta - F(q_k)\|_Y$ being the only accessible quantity during the minimization - of course, the parameter error $\|q_k - q_*\|_Q$ only is at hand in contrived examples - its monotone behavior suggests to iterate sufficiently long in order to strive for the "optimal" solution. But in fact this strategy would lead to an increase of the error in q_k with every additional iteration step due to the ill-posedness, see Figure 17. By the use of regularization methods to be outlined in the following such data error propagation effects can be avoided.

3.1.2. Variational and Iterative Regularization Though we have introduced (8) in context of the finite dimensional benchmark problem it also shall serve in the following discussion as abstract description of a general nonlinear inverse and ill-posed problem arising in systems biology. In this context, the operator F represents the map from the solution q onto the output y - to be compared with the available data y^δ - but now also might act between infinite dimensional spaces Q and Y. For inverse problems, the transition from finitely to infinitely many degrees of freedom is usually accompanied by a change from a continuous dependence of the solution on the data with large but still finite data error amplification to a discontinuous dependence with arbitrarily large error propagation. Even, in applications as described above one can easily think of sources for infinite dimensionality, e.g., if parameter constants of the ODE model are replaced by parameter functions depending on temperature, species concentrations or pH-value, or if continuous time course recordings instead of discrete time course data are considered. As a further example, (8) arises in an infinite dimensional setting if also spatial modeling aspects are taking into account by a description of the biological system in terms of partial differential equations.

If the inverse problem (8) is ill-posed in the sense that its solution (in the least squares sense) does not depend continuously on the data, algorithms tailored for well-posed problems fail if they do not address the instability, since data as well
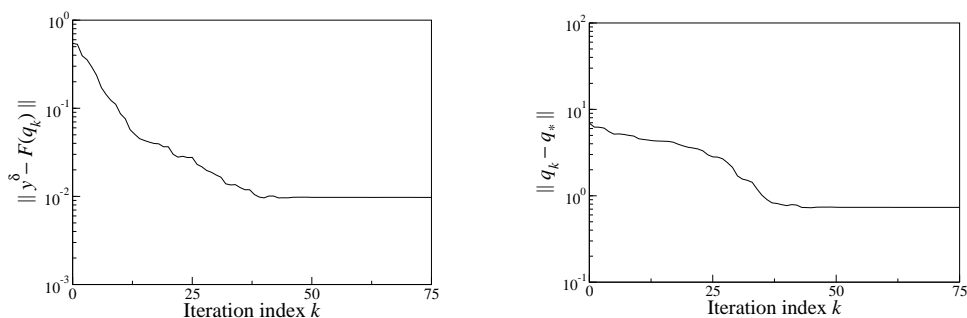
Figure 18. Course of an iterative minimization of the Tikhonov functional with $\alpha = 10^{-5}$. As opposed to the unregularized situation displayed in Figure 17, the parameter error $\|q_k - q_*\|$ decreases and stays bounded.

as round-off errors may be amplified by an arbitrarily large factor. In order to overcome these instabilities one has to use *regularization* methods, which in general terms replace an ill-posed problem by a family of neighboring well-posed problems. Among the most popular techniques are variational regularization methods where one strives for minimizers q_α^δ of functionals like

$$\|y^\delta - F(q)\|^2 + \alpha \mathcal{R}(q, q_0) \tag{12}$$

and where the purpose of the regularizing term $\mathcal{R}$ with positive regularization parameter α is to enforce stable dependency of q_α^δ on the noisy data y^δ. Here, q_0 represents an a-priori guess for the solution. Examples for common choices of $\mathcal{R}$ are

Tikhonov regularization: $\qquad \mathcal{R}(q, q_0) = \|q - q_0\|_Q^2, \tag{13a}$

maximum entropy regularization: $\quad \mathcal{R}(q, q_0) = \int_\Omega q(t) \log \frac{q(t)}{q_0(t)} \, dt, \tag{13b}$

bounded variation regularization: $\quad \mathcal{R}(q, q_0) = \int_\Omega |\nabla q(t)| \, dt, \tag{13c}$

see [40,41,117], [35,42,94] and [116,130,140], where the choice of $\mathcal{R}$ is influenced by expected or desired properties of the solution, see also below. Note that by choosing the regularization term $\mathcal{R}$ a bias may be introduced. In case of a wrongly chosen $\mathcal{R}$, (12) may lead to the best approximation of the data still compatible with $\mathcal{R}$ though the true properties of q_* are not at all reflected in the computed solution q_α^δ. The question of correctly choosing $\mathcal{R}$ cannot be solved by mathematical considerations, its answer requires practical insight into the problem.

The minimization of (12) is usually realized via iterative methods. Figure 18 illustrates the course of an iterative minimization of the Tikhonov functional, i.e., (12) with $\mathcal{R}$ as in (13a), with $\alpha = 10^{-5}$ for our benchmark parameter identification problem. As in the unregularized situation shown in Figure 17 the residual norm $\|y^\delta - F(q_k)\|$ monotonically decreases. But now, also the error in the parameter $\|q_k - q_*\|$ monotonically drops due to the use of the penalty term $\mathcal{R}$ which demonstrates that the data error propagation can be avoided by regularization.

Other preferred techniques for solving nonlinear ill-posed problems are iterative methods, see [43,82] for a comprehensive survey. Linearization of (8) at a current iterate q_k motivates the linear equation

$$F'(q_k)(q - q_k) = y^\delta - F(q_k), \tag{14}$$

whose solution q_{k+1} then should serve as a better approximation according to Newton's method. However, in the ill-posed case the operator $F'(q_k)$ is not continuously invertible so that Newton's method cannot be applied, and (14) needs to be regularized. Tikhonov regularization applied to (14) yields the Levenberg Marquardt method (see [62]) which defines q_{k+1} via

$$q_{k+1} = q_k + (F'(q_k)^*F'(q_k) + \alpha_k I)^{-1}F'(q_k)^*(y^\delta - F(q_k)), \qquad (15)$$

where α_k is a sequence of positive numbers by which the continuous invertibility of $F'(q_k)^*F'(q_k) + \alpha_k I$ is guaranteed. In the finite dimensional context, (15) with $\alpha_k = 0$ corresponds to an equation for $q_{k+1} - q_k$ involving the matrix (11). Closely related is the *iteratively regularized Gauss-Newton method* (see [6, 13])

$$q_{k+1} = q_k + (F'(q_k)^*F'(q_k) + \alpha_k I)^{-1}[F'(q_k)^*(y^\delta - F(q_k)) - \alpha_k(q_k - q_0)], \quad (16)$$

which is obtained by augmenting (15) by the term

$$-(\alpha_k I + F'(q_k)^*F'(q_k))^{-1}\alpha_k(q_k - q_0)$$

for additional stabilization. Replacing $F'(q_k)^*F'(q_k) + \alpha_k I$ in (15) by the identity mapping I (in the quasi-Newton spirit) yields the Landweber iteration

$$q_{k+1} = q_k + F'(q_k)^*(y^\delta - F(q_k)), \qquad (17)$$

a method that is slower but easier to handle, see [64]. It can also be considered as fixed point iteration applied to equation (10). More details on iterative regularization methods based on fixed point arguments can be found in [7]. For the construction of Newton-type methods based on invariance principles and on some multi-level aspects see [31].

3.1.3. Regularization Parameter In case of an ill-posed problem, an iterative method for its solution needs to be stopped "at the right time", i.e., only for a suitable stopping index k_*, the iterate $q_{k_*}^\delta$ yields a stable approximation to q_*. Otherwise, the typical semi-convergence behavior is obtained, where even as the output decreases as the iteration number increases, the error $\|q_k^\delta - q_*\|$ starts to increase after an initial decay due to the data error propagation, see our example in Figure 17.

As indicated by this example, one of the major concerns in regularization theory is how to choose the regularization parameter appropriately since its choice always reflects a compromise between accuracy and stability, see [38]. For instance, if α in (12) is chosen too large, the influence of the initial guess q_0 is too strong, leading to a poor approximation of q_*. On the other hand, if α is chosen too small, data errors may already get amplified too strongly. Hence, there always is an optimal range of regularization parameters such that with α chosen out of it an acceptable total error $\|q_\alpha^\delta - q_*\|$ can be obtained. This is also illustrated in Figure 19 for the above mentioned benchmark parameter identification problem, where the error between q_* and q_α^δ obtained by Tikhonov regularization for various values of α (but fixed data y^δ) is plotted.

In order to demonstrate the benefit of regularization with a regularization parameter within the optimal range, we have chosen $\alpha = 10^{-5}$ (close to the best choice as suggested by Figure 19) to obtain the results illustrated in Figure 18. Figure 20 gives a comparison of the corresponding regularized solution q_α^δ with the unregularized $\tilde{q}$ obtained by a pure minimization of (9). While $\tilde{q}$ shows large deviations in its components from the true solution q_*, the regularized solution q_α^δ yields a stable,
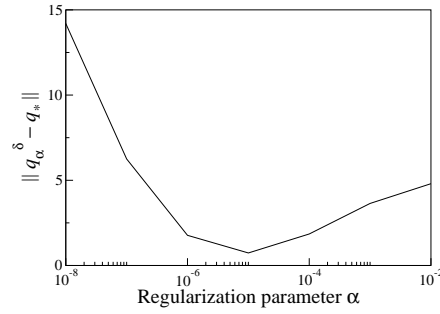
Figure 19. Total parameter error $\|q_\alpha^\delta - q_*\|$ for Tikhonov regularization in dependence on α, indicating the existence of an optimal range of regularization parameters.
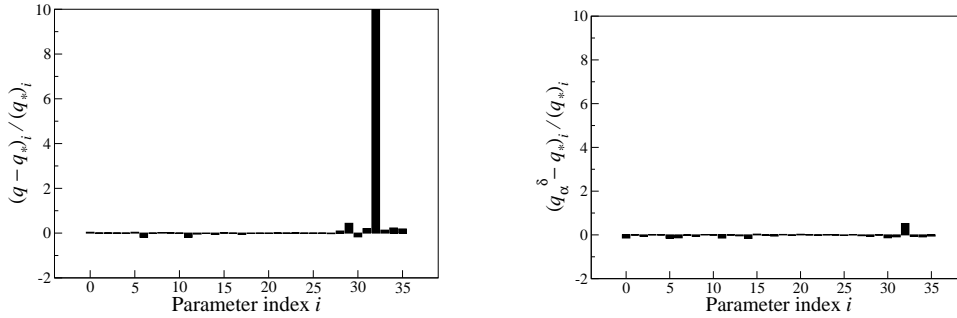

Figure 20. Individual relative errors of the identified parameters. Left: solution $\tilde{q}$ obtained via pure minimization of the data mismatch, i.e. without regularization. The relative error of parameter 32 is 3085.45 (not shown here due to the cut-off at 10). Right: solution q_α^δ obtained via Tikhonov regularization.

hence reliable approximation of q_*. Clearly, these figures only serve the purpose of illustration, since in practical problems the solution q_* for exact data is unknown and hence plots of this kind are not available. Hence, parameter choice rules have to be used in order to determine a regularization parameter which is close to the optimal one. Such strategies can be derived from theoretical analysis of the particular method under consideration.

3.1.4. Convergence Analysis and Error Concepts All regularization methods have in common that their convergence analysis is based on some knowledge about the quality of the available data y^δ. Besides stable dependency of the approximation q_α^δ (or $q_{k_*}^\delta$) on y^δ, the key attribute of regularization is a convergence property of the type

$$q_\alpha^\delta \to q^* \text{ as the quality of the data gets perfect, i.e., } \delta \to 0. \tag{18}$$

Though in the actual application the data quality is limited and cannot be driven to perfectness, theoretical (asymptotic) validation of the method is provided by (18) and guidelines for the choice of the regularization parameters can be drawn from such convergence considerations. In the deterministic, functional analysis based theory of inverse problems, see [38], the necessary data information is assumed to be given in terms of a noise level δ serving as norm bound on the data error, i.e.,

$$\|y^\delta - y\|_Y \le \delta. \tag{19}$$

Then, under additional smoothness assumptions on q_* - so-called source conditions - the goal is to derive convergence rates for the norm error between q_α^δ and q_* of the type

$$\|q_\alpha^\delta - q^*\|_Q = \mathcal{O}(f(\delta))$$

with $f(\delta) \to 0$ as $\delta \to 0$. These estimates are of a worst case type in the sense that they are valid for all noisy data compatible with (19). In many situations this is a much too restrictive way of assessing uncertainty. In particular, in biological applications information about the distribution of the data error rather than an estimate of the form (19) might be available. Motivated by statistical estimation theory, one then usually aims at estimates for the expected value of the squared norm of the deviation. For instance, if the variance $E(\|y^\delta - y\|_Y^2)$ for the data error is available, one strives for estimates for the solution error expectation $E(\|q_\alpha^\delta - q_*\|_Q^2)$. For stochastic convergence concepts in connection with inverse problems, we refer to [10, 12, 69]. For finite dimensional problems, the statistical approach to inverse problems also covers questions about confidence intervals or regions in order to determine how reliable a computed solution is. For instance, under the assumption of additive and normally distributed data noise with constant variance σ, a region around the minimizer $q_0^\delta \in \mathbb{R}^m$ of (9) can be defined in which the true solution q_* lies with a certain probability $(1 - \beta)$. Based on the Fisher information matrix $\frac{1}{\sigma^2} F'(q_0^\delta)^* F'(q_0^\delta)$, this $(1 - \beta)$ confidence region is determined by the inequality

$$(q_0^\delta - q_*)^* \left(F'(q_0^\delta)^* F'(q_0^\delta) \right) (q_0^\delta - q_*) \leq \frac{m\|y^\delta - F(q_0^\delta)\|_Y^2}{N - m} F_\beta(m, N - m),$$

where $F'(q_0^\delta) \in \mathbb{R}^{N \times m}$ and $F_\beta(m, N - m)$ is the upper β part of Fisher's distribution with m and $N - m$ degrees of freedom, see [9] for details.

In the modeling of biological phenomena, stochasticity may not only arise through the data noise but also through the model itself: frequently, one does not look for a specific quantity for a specific individual but for the distribution of the quantity over a larger population. Then, uncertainties both in the data and the unknowns can be modelled and error estimates for regularization methods can be given using the Ky Fan or the Prokhorov metric, see [39, 68]. They allow to measure distances between random variables and their distributions, respectively. Those metrics can also be used for deriving analogies to confidence intervals in an infinite-dimensional setting. Furthermore, they allow to derive convergence results for Bayesian inversion methods, see [118]. In this theory, the Bayes formula is used to derive, from available prior information and measured data, the solution of the inverse problem as posterior distribution, see [81].

3.1.5. *Parameter Choice Strategies* Returning to the actual question of regularization parameter choice, there are two general classes of strategies. While a-priori rules only involve the information about the quality of the data, a-posteriori techniques use, in addition, the actual data y^δ. Since optimal a-priori rules also require knowledge hardly accessible in applications, a-posteriori techniques, that only use available information, often are more practical. A prominent example for the latter is the discrepancy principle. In context of a deterministic analysis of variational regularization (12) it defines $\alpha = \alpha(\delta, y^\delta)$ as the solution of the nonlinear equation

$$\|F(q_\alpha^\delta) - y^\delta\| = \tau\delta \tag{20}$$

for some $\tau > 1$. In context of iterative methods, the discrepancy principle determines the regularization parameter $k_* = k_*(\delta, y^\delta)$ according to

$$\|y^\delta - F(q_{k_*}^\delta)\| \leq \tau\delta < \|y^\delta - F(q_k^\delta)\|, \quad 0 \leq k < k_*, \tag{21}$$

for some τ slightly larger than one. Hence, the iteration is stopped as soon as the residual $\|y^\delta - F(q_k^\delta)\|$ is in the order of the data error, which is somehow the best one should expect. For solving an ill-posed problem when only noisy data y^δ are given, it would make no sense to ask for an approximate solution $\tilde{q}$ with $\|y^\delta - F(\tilde{q})\| << \delta$, the price to pay would be instability, see Figure 17. While (20) requires to solve a nonlinear equation for α, with the associated theoretical questions concerning the solvability and possibly high computational effort, (21) is easy to realize. This is one reason for the attractiveness of iterative methods compared to variational regularization.

One can show (see [38]) that *error-free* strategies, where $\alpha = \alpha(y^\delta)$ (or $k_* = k_*(y^\delta)$) does not depend on δ, cannot lead to convergence as $\delta \to 0$ in the sense that $\lim_{\delta \to 0} q_\alpha^\delta = q_*$ for all y^δ satisfying (19). Since this is only an asymptotic statement, these techniques may still occasionally work well for a fixed noise level $\delta > 0$, see [63]. However, the knowledge and use of a bound δ for the data error - either deterministic or stochastic - is necessary for the construction of regularization methods based on a sound theoretical foundation. The error-free strategies include the popular methods of generalized cross-validation [159] and the *L-curve method* [65]; for its non–convergence, see [37, 158].

3.1.6. Sparsity Enforcing Regularization   Finally, we focus on the issue of sparsity enforcing regularization, as already mentioned in Section 2.2, which recently turned into an active field of research in the area of inverse problems. With respect to an underlying basis for the space Q, the principal goal is to find stable solutions q_α^δ to the inverse problem that show as few as possible deviations in its components from some reference q_0 or are sparse themselves, i.e., only possesses as few as possible components different from zero, i.e., $q_0 = 0$. In systems biology, one goal could be the infer the sparsest reaction network still compatible with the experimental data, where the components of q_α^δ then represent connections between two nodes of the network, see [89] for a study of the Chlorite Iodide reaction network. Though of chemical nature, this reaction is known to show a rich repertoire of dynamical features also encountered in biological systems such as oscillations and bistability, see [84]. Furthermore, experimental data are easier to obtain for chemical systems which makes them an attractive test case. Parameter identification in models from chemistry has been addressed earlier in the literature, [14, 15, 121], however, due to the acceptable quality of the data in the applications considered (in comparison to data in biology) the emphasis was not put on regularization.

As another example of sparsity, one might wish to influence a biological system by as few as possible interventions while achieving the desired qualitative behavior, see the examples of Section 2.3. If the system in its current state is modelled in terms of tunable reference parameters q_0, then the task is to obtain the desired system characteristics by performing as few as possible changes in q_0, see Section 3.2 for a more comprehensive discussion.

For the solution space $Q = l_p$, questions of that type can be addressed by variational regularization using the penalty term

$$\mathcal{R}(q, q_0) = \|q - q_0\|_{l_p}^p = \sum_i (q - q_0)_i^p, \ 0 < p \le 2, \tag{22}$$

where the setting $q_0 = 0$ would correspond to striving for sparsity of q_α^δ. The smaller the value of p, the closer $\mathcal{R}(q, q_0)$ approximates

$$|||q - q_0||| := \sharp \text{ of components of } (q - q_0) \text{ different from zero,} \tag{23}$$

the penalty correctly reflecting sparsity. However, since (23) is not even continuous in q, it is frequently replaced by (22) in order to avoid the high computational costs due to the use of combinatorial algorithms. For the case $p \geq 1$ several results both on theoretical and algorithmic aspects can be found in the literature, see, e.g., [28, 55, 56, 123], however, the approximation of (23) then is rather poor. The latter is improved for the choice $p < 1$, however, additional challenges in the analysis (22) then arise due to the non-convexity, the non-differentiability and the lack of norm properties of $\| \cdot \|_{l_p}$ for $p < 1$. Still, the regularization properties of (22) can be guaranteed, see [163], by using the superposition operator

$$\mathcal{N}_{p,r} : q \mapsto \varphi_{p,r}(q(\cdot)) \text{ with } \varphi_{p,r} : s \rightarrow \text{sign}(s)\,|s|^{\frac{r}{p}}$$

for $0 < p \leq 1$ and $1 \leq r \leq 2$ and the transformation

$$\tilde{q} = \mathcal{N}_{p,r}^{-1}(q) \text{ with } \|q\|_{l_p}^p \;=\; \|\mathcal{N}_{p,r}(\tilde{q})\|_{l_p}^p \;=\; \|\tilde{q}\|_{l_r}^r.$$

That way the problem formulation

$$\|y^\delta - F \circ \mathcal{N}_{p,r}(\tilde{q})\|^2 + \alpha \,\|\tilde{q} - \tilde{q}_0\|_{l_r}^r \;\rightarrow\; \min_{\tilde{q} \in l_r} \tag{24}$$

equivalent to (12) with (22) can be derived, to which standard regularization theory applies using similar proof techniques as in [41]. Current research topics include the efficient numerical solution of the minimization problem (24) and the design of iterative regularization methods that enforce sparse solutions.

3.2. Qualitative Inverse Problems

Algorithms and numerical implementations of (forward) bifurcation analysis have been developed over the past few decades and there currently exist several mature software packges in various programming languages, from `FORTRAN` [34], `C` [53,92] to `Matlab` [32,54]. In computing the bifurcation diagram, the equilibrium continuation is carried out using methods such as pseudoarclength continuation, on which bifurcation points are located via the zeros of certain test functions [54, 92]. In the state-of-the-art implementations [52, 92], limit cycle solutions are formulated as a boundary value problem (BVP) on a unit circle with the period T being a variable,

$$\begin{aligned} \dot{x}(t) - Tf(x(t), q) &= 0, \ t \in [0,1] \\ x(0) &= x(1), \Psi[x] = 0 \end{aligned} \tag{25}$$

where $\Psi[\cdot]$ is a scalar functional that enforces a *phase condition* in order to remove the rotational degree of freedom. Numerical methods for the solution of limit cycle and the detection of their bifurcations have been developed, by discretizing using the collocation method [52,93]. Once (co-dimension 1) bifurcations have been found on curves of equilibria and limit cycles, additional parameters can be freed to continue these located bifurcation points and obtain *two-parameter bifurcation diagrams*. The numerical continuation of bifurcations is carried out in an analogous manner, for instance by applying the pseudo-arclength method to *augmented systems* involving their respective defining conditions.

In application areas where nonlinear dynamics and bifurcations have traditionally played an important role, methods for the design and control of qualitative dynamics have been developed. Driven by electrical and chemical engineering problems, methods for the design of robust systems have been proposed [33, 114]: the methodology consists of finding tunable parameters that widen the regime in

the uncertain or uncontrollable parameters that maintain the same qualitative dynamical behavior. In other words, by moving the undesired bifurcation points outside the regions of operation, the stability of the system is therefore not threatened by a possible change in the qualitative dynamics. This approach has been applied to applications including avoiding voltage collapse in the electric power system [33] and improving parametric robustness in chemical reactors [114]. Methodologically, the algorithms find the closest bifurcation points and rely on gradient-based methods to place them at the desired locations. In particular, expressions for normal vectors to saddle-node and Hopf bifurcations have been derived [33, 114] as well as for bifurcations of higher co-dimensions (cusp, isola) [114]. Based on the computed vectors normal to the bifurcation manifolds, iterative methods have been derived to locate the closest bifurcation points [33] as well as provide gradient information for optimization algorithms that move these bifurcation points.

In systems biology applications, one is interested not only in questions of robustness (for instance, maximizing the parameter range that leads to oscillations about a desired period) but more generally in exploring model behavior and relating observed or desired dynamic characteristics to mechanisms. For instance, at the initial modeling stage, one may wish to explore the possibility of a given model to exhibit bistability or oscillations. Methods of computationally searching the parameter space for different qualitative dynamics have been proposed, using either genetic algorithms [19] or carrying out lift-and-project iterations for the respective inverse eigenvalue problems [103]. We note that in many modeling applications, one wishes not only to probe the possibility of a model to exhibit a particular behavior but also to identify the underlying mechanisms; for addressing such questions, the use of sparsity enforcing regularization is crucial [103, 104].

At the initial modeling stage, the task of placing bifurcation points at specific locations is of practical importance as well. As an example from circadian rhythm modeling [23], using the initial parameter estimates it was found (by carrying out a bifurcation analysis with respect to the Hill coefficient n) that oscillations can only occur at an unrealistically high value of $n = 32$. The question is then: can one identify a set of parameters such that the Hopf bifurcation occurs at the value $n = 4$? Using genetic algorithm, this problem has been addressed in [23].

In this section, we consider qualitative inverse problems under sparsity enforcing regularization formulated as the following constrained minimization problem,

$$\|y - F(q)\|^2 + \alpha l_{p,\epsilon}(\frac{q - q_0}{q^0}) \to \min_q, \quad g(q) \geq 0, \tag{26}$$

where $g(q)$ denote possible inequality constraints that may arise, α the regularization parameter and

$$l_{p,\epsilon}(x) = \sum_i (x_i^2 + \epsilon)^{p/2} \tag{27}$$

is the sparsity enforcing penalty with a smoothing parameter ϵ; refer to Figure 21 for an illustration. We note that the functional is only convex within the box $\{x : |x| \leq \sqrt{\epsilon}\}$; thus, the value of $\sqrt{\epsilon}$ could serve as a threshold for classifying parameters as having been identified by the algorithm. In all the numerical examples shown in this section, we have chosen $\epsilon = 10^{-2}$. We remark that an evaluation of the forward operator, $F(q)$, entails computing the bifurcation diagram of the system of interest with respect to some chosen bifurcation parameter(s). Computationally, this would entail carrying out pseudo-arclength continuation using Newton's method and/or solving the BVP (25). In the numerical examples below, the misfit term $\|y - F(q)\|$ might represent the distance of some bifurcation points to their desired
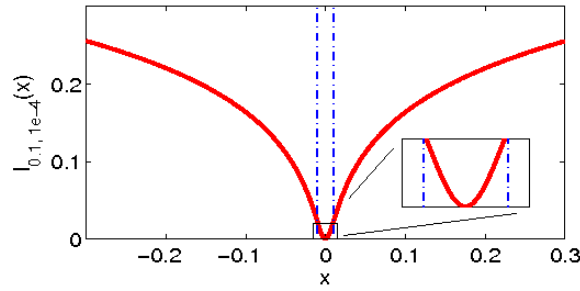
Figure 21. Smoothed sparsity enforcing penalty (27): $p = 0.1, \epsilon = 10^{-4}$

(a) Initial oscillatory domain in (α, β)-plane
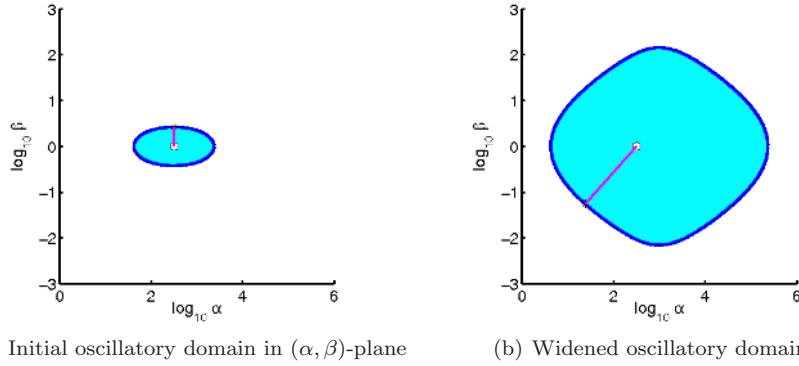
(b) Widened oscillatory domain

Figure 22. Design of an oscillatory domain

locations, or some performance measure of the dynamic characteristics such as the deviation of the period of the limit cycle oscillation from the desired value.

As a simple instance, consider the situation where one has a model which gives rise to the desired dynamic behavior but one would like to widen the parameter regime which leads to the same qualitative dynamics. In this case, the term $\|y - F(q)\|$ measures the distance of the nearest bifurcation manifold from the nominal parameters, y. We take as the model system the 3-gene repressilator [115] in which the interaction graph of the genes forms a ring whereby each gene represses the next one, modelled by the following ODE system:

$$
\begin{aligned}
\dot{x}_i &= \beta_i(y_i - x_i) \\
\dot{y}_i &= \alpha_i \left(\frac{1 - \delta_i}{1 + x_{(i-1)| \mod 3}^{h_i}} + \delta_i \right) - y_i, \ i = 0, \cdots, 2.
\end{aligned}
$$

In Figure 22, we show that by applying the algorithm developed for solving (26) to the repressilator system, the oscillatory domain in the (α, β)-plane can be maximized [105]. As another example on increasing robustness, we discuss in Section 3.2.3 a problem involving a circadian rhythm model where the goal is to maintain constancy of period over a range parameter values.

In the following subsections, we show a number of qualitative inverse problems which can be formulated as (26), illustrating some possible applications in designs and therapeutics. In Section 3.2.1, we look at transformations of the bifurcation diagram as shown in Figure 8 as a way to reverse-engineer the network and deduce the

important interactions underlying the observed bifurcation phenotype. In solving such reverse-engineering problems, sparsity-promoting regularization is important in order to derive solutions that are more useful in the biological context [104]. As an example of the inverse qualitative problems that arise in identifying mechanisms for possible therapeutic treatments, we discuss in Section 3.2.2 an example involving a Hypothalamic-Pituitary-Adrenal (HPA) axis model, showing how sparsity penalty can be used to identify important interactions in the network which could serve as possible drug targets. Lastly, in Section 3.2.3 we show a design example where we would like to tune parameters in a circadian rhythm model such that the period of oscillation is robust with respect to a loosely regulated parameter.

3.2.1. Numerical example: G_1/S transition In this example, we go back to the example first shown in Section 2.3.1, whose full ODE system is shown in Appendix D. We ask: given that the location of the saddle-node bifurcation points has important physiological implications, what network components (or 'knobs') could tuned to give rise to the geometric transformations as depicted in Figure 9?

To solve such inverse bifurcation problems, we formulate them as constrained optimization problems of the following form: over the set of system parameters q_s, minimize the non-convex penalty function $l_{p,\epsilon}(\cdot)$ under the constraints on the location of the saddle-node bifurcation points:

$$\min_{q_s} l_{p,\epsilon}\left(\frac{q_s - q_s^*}{q_s^*}\right) \text{ subject to } \begin{cases} \mathrm{SN}_1(q_s) = \mathrm{SN}_1^*, \\ \mathrm{SN}_2(q_s) = \mathrm{SN}_2^*. \end{cases} \tag{28}$$

In particular, we considered the 3 modes of bifurcation phenotype given in Figure 9. Using the sparsity-promoting penalty, the computational results point to a core part of the network, consisting of 2 genes, that control the bifurcation phenotype of the network [104]. The effect of the choice of penalty term is illustrated in Figure 23: while both solutions give rise to the same specified shift in the bifurcation points, the l_2 result would be much more challenging to interpret in the biological context.

3.2.2. Numerical example: stress response in HPA axis In this example, we examine a model of the Hypothalamic-Pituitary-Adrenal (HPA) axis [60], which play an important role in maintaining body homeostasis in response to various stresses. For some parameter values, the model predicts the bistability in the solution: once a sufficiently high stress level has been reached, the systems lies permanently in an elevated response state even after the stress level has been removed. Physiologically, this could correspond to a *chronic stress condition*. A simulation of the model that corresponds to such a condition is shown in the middle column of Figure 24: once the amplitude of the stress pulse (shown as gray blocks) goes above 0.25, the system does not go back to the low response state. Given this behavior, we ask the following question: which mechanisms could delay the onset of chronic stress condition, to a higher stress level? The corresponding inverse bifurcation problem is to shift the saddle-nodes (or limit-points) as shown in Figure 25. Using the sparsity-promoting penalty, a change in 2 parameters has been identified, giving rise to the model behavior shown in the right column of Figure 24: we see that the HPA response remains reversible for the stress level 0.25, successfully delaying the chronic condition to a higher input stress level. Finally, we note that the use of sparsity promoting penalty is important for obtaining results that are more easily interpretable in the biological context: Figure 26 shows that in comparison, the result obtained using a sparsity enforcing penalty $l_{p,\epsilon}$, see (27), is more useful than the standard l_2-penalty because it identifies a few especially relevant parameters.
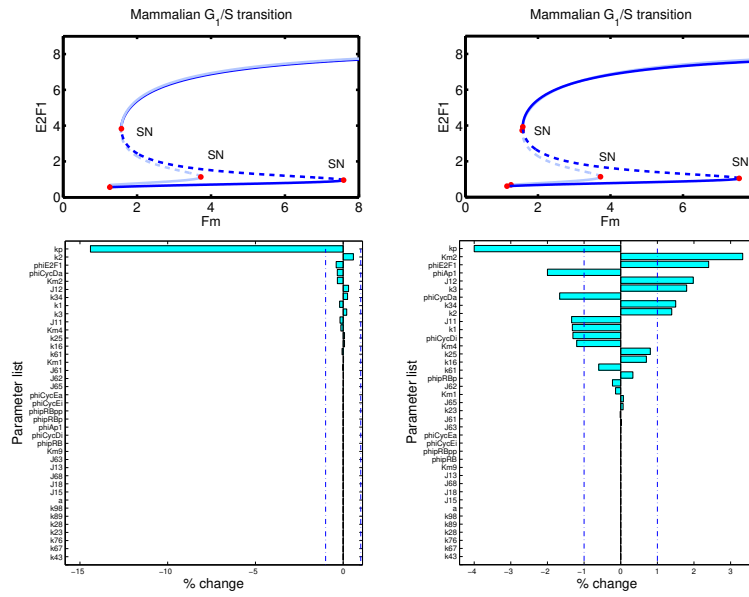
(a) Sparsity-promoting $l_{p,\epsilon}$ functional

(b) Standard l_2 functional

Figure 23. Identified parameters leading to elongating saddle-nose using l_p and l_2 penalty functions
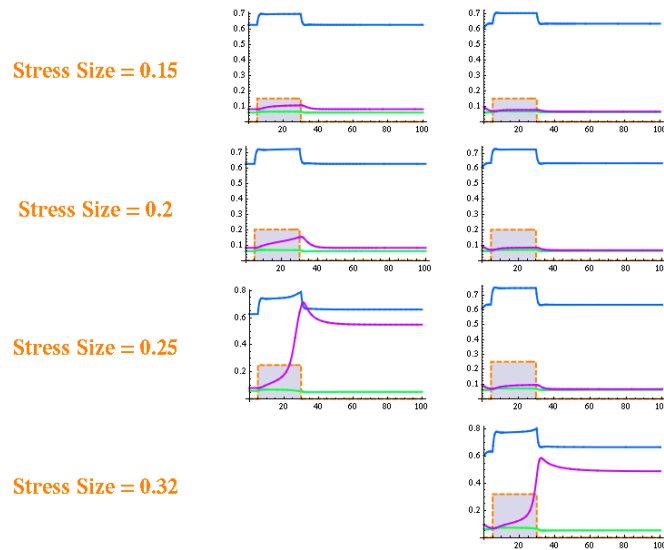

Figure 24. Delay of chronic stress in the HPA axis model: the irreversible system response in the left column is delayed to a higher stress level, as shown in the right column
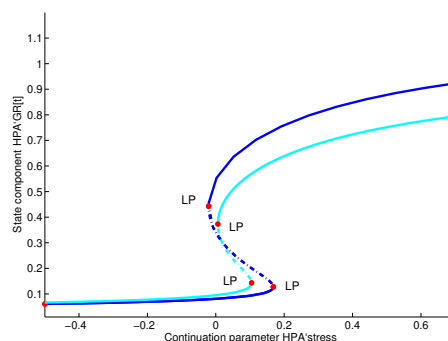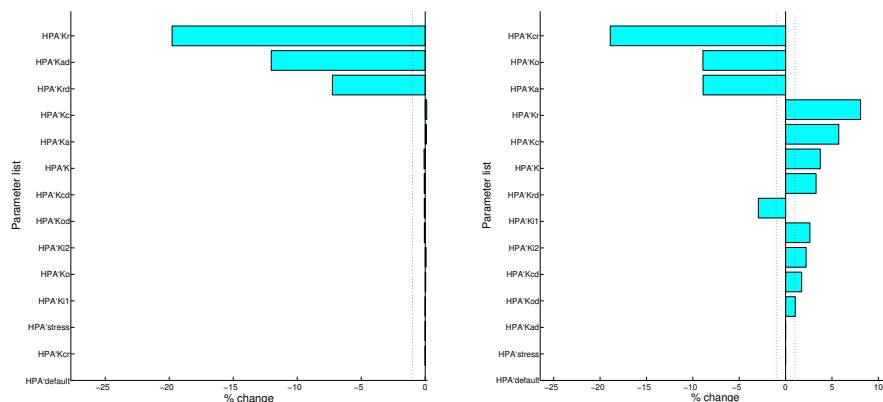
Figure 25. Shifting the saddle-node in the HPA axis model

(a) Sparsity-promoting $l_{p,\epsilon}$ penalty

(b) Standard l_2 functional

Figure 26. Identified stress-relieving parameters using different penalty functions

3.2.3. Numerical example: circadian rhythm As is mentioned in Section 2.3.2, period robustness is an important dynamical feature of circadian rhythm models. Here, we look at a circadian rhythm model in *Drosophila* proposed by Leloup and Goldbeter [97]; see Appendix D for the full system of equations). In particular, we formulate an inverse problem regarding period robustness under parametric variation. In many gene regulatory systems, the degradation rates of mRNA and proteins are not regulated and can undergo large fluctuations. In the following test case, we consider the maximum degradation rate of the TIM mRNA, v_{mT} (highlighted in the ODE system shown in Appendix D) and ask if one can fine-tune the model such that it exhibits robust oscillation period within some range of values of v_{mT}. Show in Figure 27 is the bifurcation diagram of the model with respect to v_{mT}, showing that within the parameter window $0.4 \leq v_{mT} \leq 1$ there exists a stable limit cycle solution whose period of oscillations (bottom plot) exhibits some variation from 24-hour. As a measure of period robustness, the *total variation* functional may be an appropriate choice. Hence, to identity parameters resulting in period robustness, we formulate the following minimization problem:

$$\min_{q} J(q) = TV(\text{period}(q) - 24hr) + \alpha l_{p,\epsilon}\left(\frac{q - q^*}{q^*}\right)$$
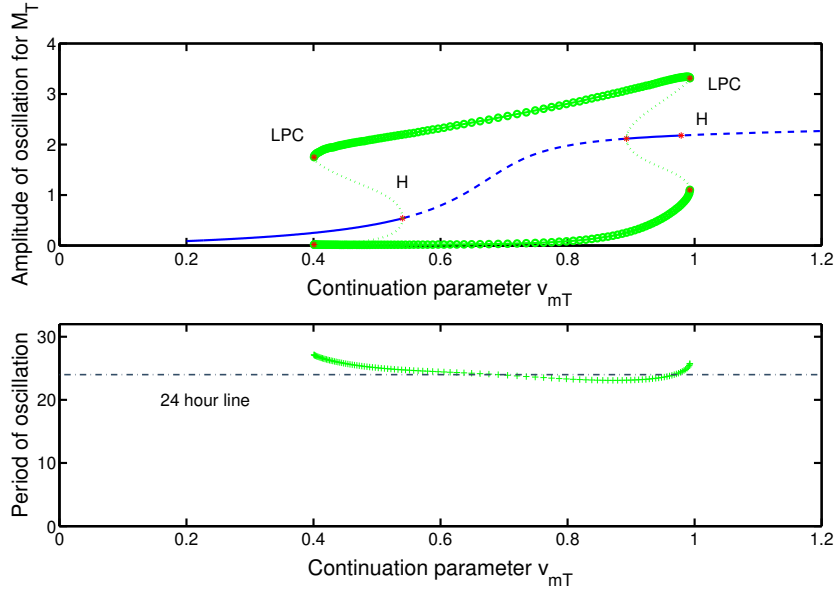
Figure 27. Bifurcation diagram in the circadian rhythm model with respect to the parameter v_{mT}: original parameter settings

$$s.t. \qquad \mathrm{LPC}_{\mathrm{left}}(q) \geq \mathrm{LPC}_L$$
$$\mathrm{LPC}_{\mathrm{right}}(q) \leq \mathrm{LPC}_U,$$

where constraints are imposed on the lower and upper values of the Limit Point of Cycles (LPC) so as to ensure that oscillations occur within the desired window of values for v_{mT}. We solve the above minimization problem with the regularization parameter value of $\alpha = 10^{-4}$, obtaining the solution shown in Figure 28. It can be seen that the period variation within the high-lighted window has been essentially eliminated. Furthermore, the use of sparsity regularization again gives a sparser result compared to that obtained using the l_2 regularization; see Figure 29. The species involved in the identified mechanisms are highlighted in Figure 30.

4. Outlook

In this paper we illustrated the importance of regularization for the stable treatment both of parameter identification and of qualitative inverse problems originating from systems biology. The illustrating examples – and similar problems we so far worked on – are of a much lower dimension than in realistic systems biology applications, where the number of variables in the ODEs might be several thousands. Also, the number of parameters might be of the same order of magnitude if not even higher, which increases the instability of the inversion problems. This situation will require both upscaling and new strategies: for the inverse problems, multi-level approaches taking into account already known modular structures will be useful. On the other hand, sparsity enforcing techniques may be suitable for finding unknown modular structures, providing thereby alternative appproaches to other techniques reducing the number of variables, for examples stationarity of intermediates or reduction of complex reaction mechanisms, see [128]. Also, (mathematical) model reduction, where a large (differential equation) system is replaced by a smaller surrogate model, use inverse problems techniques for determining the parameters in the latter, see, e.g., [11] and [30].
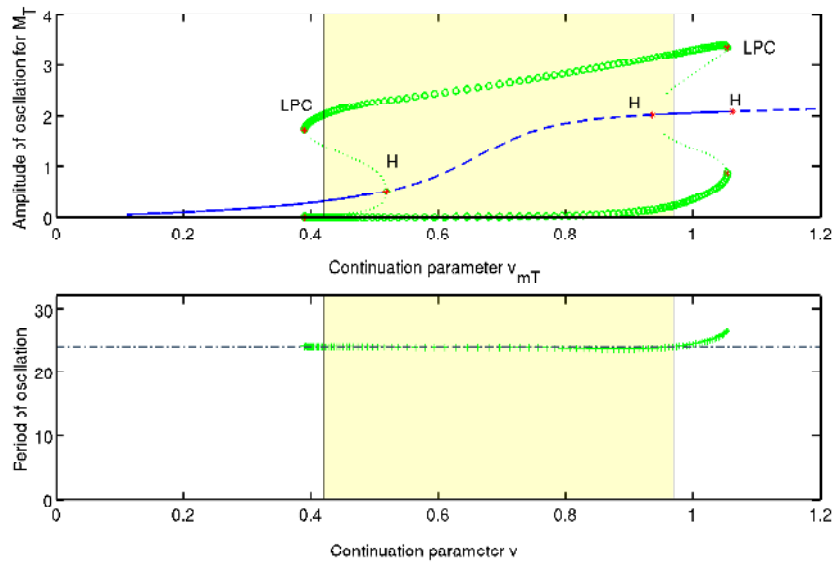
Figure 28. Bifurcation diagram in the circadian rhythm model with respect to the parameter v_{mT}: optimized parameters
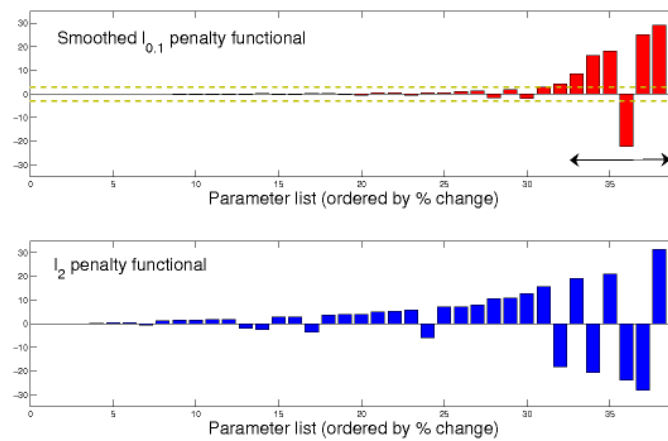
Figure 29. Effectiveness of sparsity-promoting regularization in the circadian rhythm example

Cells and organisms have also rich spatial structures that are largely neglected by ODE models. Both experimental and mathematical techniques have to be further developed to cope with this aspect. Finally, stochastic effects play a role because of low particle numbers or environmental fluctuations. For dealing with these challenges, appropriate forward models and solvers will have to be developed further; for large scale inverse problems, an optimal interplay and coupling between forward, adjoint and inverse solvers is decisive for computational tractability and efficiency. Guidance might be taken from techniques and results for the identification of distributed parameters in partial differential equations where the (discretized) inverse problems are high-dimensional by nature.

Figure 30. Species involved in the identified mechanisms from the circadian rhythm example

Appendix A

In this appendix, we elaborate on the simple reaction network which is used in the introduction to explain the concepts of *metabolic pathway analysis* and *chemical reaction network theory*. This mechanism lies at the heart of the cell cycle model, discussed in further detail in Appendix C.

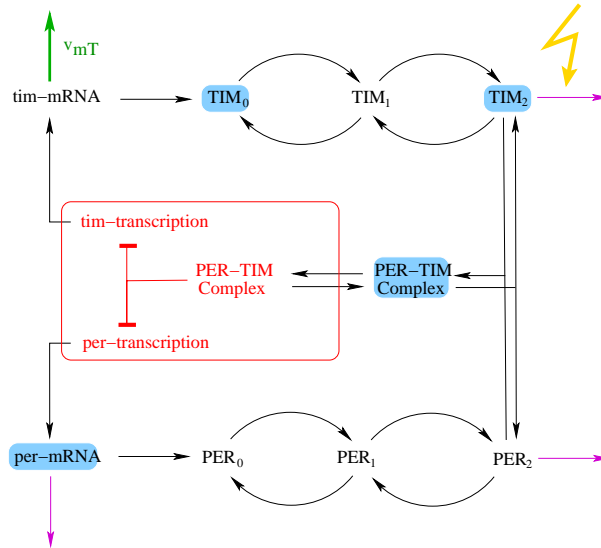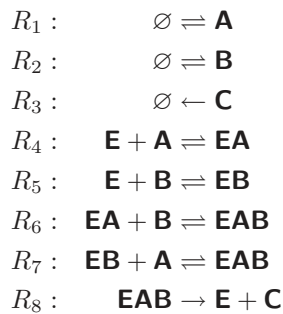We consider a reaction network involving 7 chemical species and 8 chemical reactions: $\mathcal{S} = \{\mathbf{A}, \mathbf{B}, \mathbf{C}, \mathbf{E}, \mathbf{EA}, \mathbf{EB}, \mathbf{EAB}\}$ and $\mathcal{R} = \{R_1, R_2, R_3, R_4, R_5, R_6, R_7, R_8\}$, where

$$
\begin{aligned}
R_1 : &\quad \varnothing \rightleftharpoons \mathbf{A} \\
R_2 : &\quad \varnothing \rightleftharpoons \mathbf{B} \\
R_3 : &\quad \varnothing \leftarrow \mathbf{C} \\
R_4 : &\quad \mathbf{E} + \mathbf{A} \rightleftharpoons \mathbf{EA} \\
R_5 : &\quad \mathbf{E} + \mathbf{B} \rightleftharpoons \mathbf{EB} \\
R_6 : &\quad \mathbf{EA} + \mathbf{B} \rightleftharpoons \mathbf{EAB} \\
R_7 : &\quad \mathbf{EB} + \mathbf{A} \rightleftharpoons \mathbf{EAB} \\
R_8 : &\quad \mathbf{EAB} \rightarrow \mathbf{E} + \mathbf{C}
\end{aligned}
$$

Reactions $R_1 - R_3$ denote the exchange of species $\mathbf{A}, \mathbf{B}, \mathbf{C}$ with the environment, whereas $R_4 - R_8$ are internal. Most reactions are reversible, whereas R_3, R_8 are irreversible.

This system can be seen as a (small) metabolic pathway, which transforms $\mathbf{A}, \mathbf{B}$ into $\mathbf{C}$ via several enzymatic reactions. As the notation suggests, the system can also be seen as a mechanism for a single enzyme with unordered substrate binding. In

this view, enzyme **E** has substrates **A**, **B** and product **C** and can form the enzyme-substrate-complex **EAB** in two different orders: via **EA** or **EB**.

In the metabolic pathway approach, the stoichiometric matrix S of a reaction network is assumed to be known, whereas the corresponding rate laws $v(x, q)$ are unknown. The resulting ODE system is written as $\dot{x} = Sv(x, q)$. In our example, we have:

$$\frac{d}{dt}\begin{pmatrix} x_A \\ x_B \\ x_C \\ x_E \\ x_{EA} \\ x_{EB} \\ x_{EAB} \end{pmatrix} = \begin{pmatrix} +1 & 0 & 0 & -1 & 0 & 0 & -1 & 0 \\ 0 & +1 & 0 & 0 & -1 & -1 & 0 & 0 \\ 0 & 0 & -1 & 0 & 0 & 0 & 0 & +1 \\ 0 & 0 & 0 & -1 & -1 & 0 & 0 & +1 \\ 0 & 0 & 0 & +1 & 0 & -1 & 0 & 0 \\ 0 & 0 & 0 & 0 & +1 & 0 & -1 & 0 \\ 0 & 0 & 0 & 0 & 0 & +1 & +1 & -1 \end{pmatrix} \begin{pmatrix} v_1(x_A, q) \\ v_2(x_B, q) \\ v_3(x_C, q) \\ v_4(x_A, x_E, x_{EA}, q) \\ v_5(x_B, x_E, x_{EB}, q) \\ v_6(x_B, x_{EA}, x_{EAB}, q) \\ v_7(x_A, x_{EB}, x_{EAB}, q) \\ v_8(x_{EAB}, q) \end{pmatrix}$$

Remark: Of course, there could be stoichiometric coefficients other than ± 1. E.g., a reaction $\mathbf{A} + 2\mathbf{B} \rightleftharpoons \mathbf{C}$ would yield a column $(-1, -2, +1, 0, 0, 0, 0)^T$ in the stoichiometric matrix.

Lacking information on the rate laws, one cannot analyze the dynamical behavior of the system. However, one may ask what steady states are accessible to the system. A steady state flux v is characterized by $0 = Sv$ and $v_i \geq 0$ if R_i is irreversible. More specifically one may ask what are the *elementary flux modes*. An elementary flux mode e fulfills the steady state condition, i.e. $0 = Se$, and the feasibility condition, i.e. $e_i \geq 0$ if R_i is irreversible. Another condition, called non-decomposability, guarantees a minimal (and unique) set of elementary flux modes [143,144]. As a consequence, any steady state flux can be written (in a non-unique way) as a nonnegative combination of elementary flux modes: $v = \sum_j \alpha_j e^j$, $\alpha_j \geq 0$. Mathematically speaking, the admissible fluxes are restricted to a convex polyhedral cone whose generating vectors (extreme rays) are contained in the set of elementary flux modes. The concept of *extreme pathways* is another variant of this approach [141].

In our example, the elementary flux modes can be computed to be:

$$e^1 = \begin{pmatrix} 1 \\ 1 \\ 1 \\ 1 \\ 0 \\ 1 \\ 0 \\ 1 \end{pmatrix}, \quad e^2 = \begin{pmatrix} 1 \\ 1 \\ 1 \\ 0 \\ 1 \\ 0 \\ 1 \\ 1 \end{pmatrix}, \quad e^3 = \begin{pmatrix} 0 \\ 0 \\ 0 \\ +1 \\ -1 \\ +1 \\ -1 \\ 0 \end{pmatrix}, \quad e^4 = \begin{pmatrix} 0 \\ 0 \\ 0 \\ -1 \\ +1 \\ -1 \\ +1 \\ 0 \end{pmatrix} \tag{29}$$

Pathway analysis aims at decomposing large reaction networks into smaller functional modules. Elementary flux modes represent all routes that enable a reaction network (e.g. a metabolism) to transform certain substrates into a product. In our example, flux modes e^1 and e^2 correspond to the sub-networks $\{R_4, R_6, R_8\}$ and $\{R_5, R_7, R_8\}$ (combined with the exchange reactions $\{R_1, R_2, R_3\}$). On the other hand, flux modes e^3 and e^4 involve only the internal sub-network $\{R_4, R_5, R_6, R_7\}$ and do not transform substrates into product. They are so-called futile cycles and do not perform a biochemically meaningful function. (The corresponding species-reaction graphs are depicted in Figure 31.)

Remark: When the reaction network is viewed as an enzyme mechanism for unordered substrate binding, the result of pathway analysis just confirms the fact
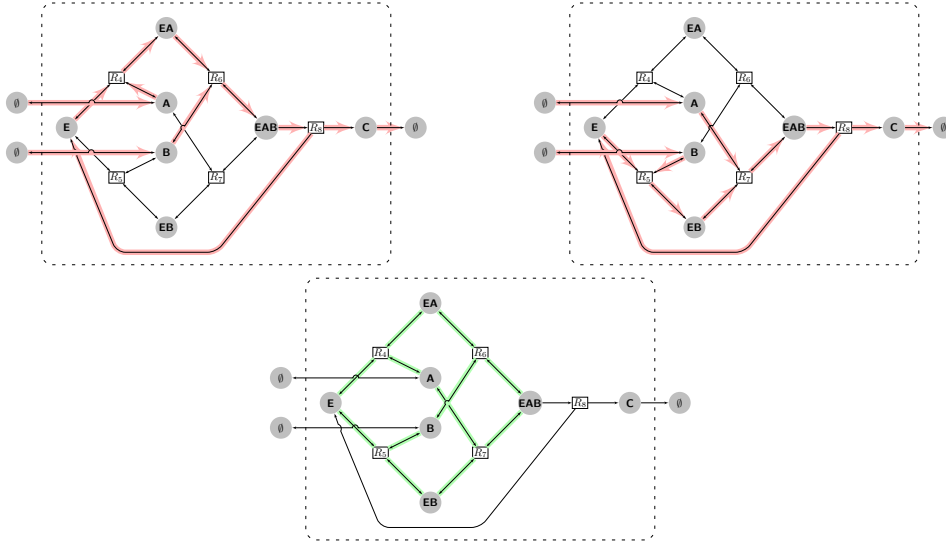
Figure 31. The two major elementary flux modes through the example network (top left and right panel) and the futile cycle (lower panel). Note that the futile cycle can operate in both directions.

that the internal overall reaction $\mathbf{A}+\mathbf{B} \rightarrow \mathbf{C}$ is a combination of the two mechanisms for ordered substrate binding $\mathbf{E} + \mathbf{A} + \mathbf{B} \rightleftharpoons \mathbf{EA} + \mathbf{B} \rightleftharpoons \mathbf{EAB} \rightarrow \mathbf{E} + \mathbf{C}$ and $\mathbf{E} + \mathbf{A} + \mathbf{B} \rightleftharpoons \mathbf{EB} + \mathbf{A} \rightleftharpoons \mathbf{EAB} \rightarrow \mathbf{E} + \mathbf{C}$. For the study of enzyme mechanisms, but also of metabolic, genetic, or signal-transduction networks, the approach of chemical reaction network theory may yield more significant results.

As opposed to metabolic pathway analysis, chemical reaction network theory (CRNT) does not consider overall enzymatic reactions with unknown rate laws. In CRNT, reactions are assumed to be elementary and rate laws are determined by mass-action kinetics. However, the values of the rate constants need not be known. Still, one can do useful analysis of the dynamical system. For example one may ask, if there are rate constants – represented by the parameter vector q – such that the dynamical system $\dot{x} = Sv(x, q)$ admits multiple steady states, i.e. if there exist q and $x^1 \neq x^2$ such that $0 = Sv(x^1, q)$ and $0 = Sv(x^2, q)$. This problem is particularly interesting since the existence of multiple steady states in a dynamical model of a biological cell is believed to capture the phenomenon of cell differentiation [153], i.e. the ability of a cell to operate in different modes depending on its history and its environment. One may also ask, if there are rate constants such that the dynamical system is able to oscillate.

In our example, the ODE system under the assumption of mass action kinetics amounts to:

$$
\frac{d}{dt}\begin{pmatrix} x_A \\ x_B \\ x_C \\ x_E \\ x_{EA} \\ x_{EB} \\ x_{EAB} \end{pmatrix} = \begin{pmatrix} +1 & 0 & 0 & -1 & 0 & 0 & -1 & 0 \\ 0 & +1 & 0 & 0 & -1 & -1 & 0 & 0 \\ 0 & 0 & -1 & 0 & 0 & 0 & 0 & +1 \\ 0 & 0 & 0 & -1 & -1 & 0 & 0 & +1 \\ 0 & 0 & 0 & +1 & 0 & -1 & 0 & 0 \\ 0 & 0 & 0 & 0 & +1 & 0 & -1 & 0 \\ 0 & 0 & 0 & 0 & 0 & +1 & +1 & -1 \end{pmatrix} \begin{pmatrix} k_1 - k_{-1} \cdot x_A \\ k_2 - k_{-2} \cdot x_B \\ k_{-3} \cdot x_C \\ k_4 \cdot x_E \cdot x_A - k_{-4} \cdot x_{EA} \\ k_5 \cdot x_E \cdot x_B - k_{-5} \cdot x_{EB} \\ k_6 \cdot x_{EA} \cdot x_B - k_{-6} \cdot x_{EAB} \\ k_7 \cdot x_{EB} \cdot x_A - k_{-7} \cdot x_{EAB} \\ k_8 \cdot x_{EAB} \end{pmatrix}
$$

For example, the rate law of the reversible reaction R_4 is given by $v_4(x_A, x_E, x_{EA}, q) = k_4 \cdot x_E \cdot x_A - k_{-4} \cdot x_{EA}$, which is the difference of the mass action terms for the forward and backward direction.

But there is even more structure in the ODE system for a chemical reaction network with mass-action kinetics. To see this, we introduce the concept of *chemical complexes*, which are the left-hand-sides and right-hand-sides of the chemical reactions. The set of complexes may include the zero complex, individual chemical species, or sums of species. In our example, we have 12 complexes: $\mathcal{C} = \{\varnothing, \mathbf{A}, \mathbf{B}, \mathbf{C}, \mathbf{EA}, \mathbf{EB}, \mathbf{EAB}, \mathbf{E} + \mathbf{A}, \mathbf{E} + \mathbf{B}, \mathbf{EA} + \mathbf{B}, \mathbf{EB} + \mathbf{A}, \mathbf{E} + \mathbf{C}\}$.

The graph of chemical complexes depicts which complexes are connected by a reaction. In our example, we have:

$$
\mathbf{C}
$$
$$
\downarrow
$$
$$
\mathbf{A} \leftrightharpoons \varnothing \rightleftharpoons \mathbf{B}
$$

$$
\mathbf{E} + \mathbf{A} \rightleftharpoons \mathbf{EA} \quad \mathbf{EB} \leftrightharpoons \mathbf{B} + \mathbf{E}
$$

$$
\mathbf{EA} + \mathbf{B} \rightleftharpoons \mathbf{EAB} \leftrightharpoons \mathbf{A} + \mathbf{EB}
$$
$$
\downarrow
$$
$$
\mathbf{E} + \mathbf{C}
$$
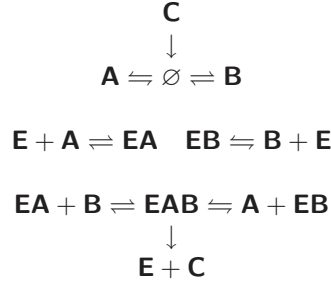
Using this concept, the dynamical system can be written in the form $\dot{x} = \Gamma A_q \Psi(x)$, where $\Psi : \mathbb{R}^{\mathcal{S}} \to \mathbb{R}^{\mathcal{C}}$ is a non-linear mapping from the vector space of chemical species $\mathbb{R}^{\mathcal{S}}$ to the vector space of chemical complexes $\mathbb{R}^{\mathcal{C}}$ and where $A_q : \mathbb{R}^{\mathcal{C}} \to \mathbb{R}^{\mathcal{C}}$ and $\Gamma : \mathbb{R}^{\mathcal{C}} \to \mathbb{R}^{\mathcal{S}}$ are linear mappings. To be more specific, Ψ assigns to a species vector the corresponding "occupation numbers" of the chemical complexes, the square matrix A_q (with rate constants as entries) determines the interactions between complexes, and Γ assigns to a complex vector the stoichiometric coefficients of the chemical species involved.

In our example, we have:

$$
\frac{d}{dt}
\begin{pmatrix}
x_A \\
x_B \\
x_C \\
x_E \\
x_{EA} \\
x_{EB} \\
x_{EAB}
\end{pmatrix}
= \Gamma A_q
\begin{pmatrix}
1 \\
x_A \\
x_B \\
x_C \\
x_{EA} \\
x_{EB} \\
x_{EAB} \\
x_E \cdot x_A \\
x_E \cdot x_B \\
x_{EA} \cdot x_B \\
x_{EB} \cdot x_A \\
x_E \cdot x_C
\end{pmatrix}
$$

with

$$
\Gamma =
\begin{pmatrix}
0 & 1 & 0 & 0 & 0 & 0 & 0 & 1 & 0 & 0 & 1 & 0 \\
0 & 0 & 1 & 0 & 0 & 0 & 0 & 0 & 1 & 1 & 0 & 0 \\
0 & 0 & 0 & 1 & 0 & 0 & 0 & 0 & 0 & 0 & 0 & 1 \\
0 & 0 & 0 & 0 & 0 & 0 & 0 & 1 & 1 & 0 & 0 & 1 \\
0 & 0 & 0 & 0 & 1 & 0 & 0 & 0 & 0 & 1 & 0 & 0 \\
0 & 0 & 0 & 0 & 0 & 1 & 0 & 0 & 0 & 0 & 1 & 0 \\
0 & 0 & 0 & 0 & 0 & 0 & 1 & 0 & 0 & 0 & 0 & 0
\end{pmatrix}
$$

and

$$A_q = \begin{pmatrix}
-(k_1+k_2) & k_{-1} & k_{-2} & k_{-3} & 0 & 0 & 0 & 0 & 0 & 0 & 0 & 0 \\
k_1 & -k_{-1} & 0 & 0 & 0 & 0 & 0 & 0 & 0 & 0 & 0 & 0 \\
k_2 & 0 & -k_{-2} & 0 & 0 & 0 & 0 & 0 & 0 & 0 & 0 & 0 \\
0 & 0 & 0 & -k_{-3} & 0 & 0 & 0 & 0 & 0 & 0 & 0 & 0 \\
0 & 0 & 0 & 0 & -k_{-4} & 0 & 0 & k_4 & 0 & 0 & 0 & 0 \\
0 & 0 & 0 & 0 & 0 & -k_{-5} & 0 & 0 & k_5 & 0 & 0 & 0 \\
0 & 0 & 0 & 0 & 0 & 0 & -(k_{-6}+k_{-7}+k_8) & 0 & 0 & k_6 & k_7 & 0 \\
0 & 0 & 0 & 0 & k_{-4} & 0 & 0 & -k_4 & 0 & 0 & 0 & 0 \\
0 & 0 & 0 & 0 & 0 & k_{-5} & 0 & 0 & -k_5 & 0 & 0 & 0 \\
0 & 0 & 0 & 0 & 0 & 0 & k_{-6} & 0 & 0 & -k_6 & 0 & 0 \\
0 & 0 & 0 & 0 & 0 & 0 & k_{-7} & 0 & 0 & 0 & -k_7 & 0 \\
0 & 0 & 0 & 0 & 0 & 0 & k_8 & 0 & 0 & 0 & 0 & 0
\end{pmatrix}$$

Remark: The interaction matrix has zero row sum. More specifically, every diagonal entry is the negative sum of the other entries in this column.

Now, we return to the question of multiple steady states. From $\dot{x} = \Gamma A_q \Psi(x)$ we see that steady states may be solutions of either $0 = A_q \Psi(x)$ or $0 \neq A_q \Psi(x)$ and $0 = \Gamma A_q \Psi(x)$. The *deficiency* of a reaction network quantifies the extent of the second possibility. It is defined as $\delta = \dim(\mathrm{Ker}\,\Gamma \cap \mathrm{Im}\,A_q)$. Under certain conditions [59], it can be shown that $\delta = m - l - s$, where m is the number of chemical complexes, l is the number of linkage classes (connected components in the graph of chemical complexes), and s is the number of linear independent reactions (the rank of the stoichiometric matrix).

In particular, one is interested in positive steady states, i.e. vectors with only positive components. The *deficiency zero theorem* states that chemical reaction networks with deficiency zero have at most one positive steady state, which – if it exists – is asymptotically stable. For networks with deficiency zero, the theorem rules out the possibility of multiple positive steady states and also oscillations. The theorem is particularly important, since many natural as well as engineered systems have deficiency zero. See e.g. [133].

In our example, the deficiency amounts to $\delta = 12 - 4 - 6 = 2$, since we have 12 chemical complexes, 4 linkage classes in the graph, and 6 linear independent reactions. Hence, the deficiency zero condition is not met, and bistability is not ruled out. In fact, it can be shown that there is a parameter vector q such that the reaction network has two positive steady states, i.e. the system can be bistable [25].

Appendix B

In the following, we present the metabolic pathway model depicted in Figure 32, which has been used as a benchmark problem in [113, 126]. The model describes the transformation of substrate S into product P via the intermediate metabolites M1, M2. The enzymes E1, E2, E3 catalyzing the transformation (and the corresponding mRNAs G1, G2, G3) are produced by 3 genes, which in turn are regulated by the metabolites. The regulation involves activation as well as inhibition.

The ODE system describing the dynamics of the model contains 8 variables, 36 parameters, and 2 experimental settings. It is given in Table 1(a). The 8 ODE variables are the concentrations of the mRNAs, enzymes, and metabolites. Using the notation of Section 2.1, we write $x = (G_1, G_2, G_3, E_1, E_2, E_3, M_1, M_2)$. The corresponding initial values are given in Table 1(b). The 36 parameters can be divided into the following classes: transcription/translation rates V, equilibrium constants K, Hill coefficients n, degradation rates k, and catalytic constants k_{cat}. We write $q = (V_1, K_{i1}, n_{i1}, K_{a1}, n_{a1}, k_1, \ldots, k_{cat3}, K_{m5}, K_{m6})$. Their true values (used for generating the experimental data) are listed in Table 1(c). The concentrations of substrate and product are constant in time, but they serve as experimental settings. 4 concentrations of S and P, respectively, have been used

<table>
<tr><td colspan="5">(c) Parameters</td></tr>
</table>

#	name	q_*	q_{lb}	q_{ub}
0	V_1	1	10^{-6}	10^{+6}
1	K_{i1}	1	10^{-6}	10^{+6}
2	n_{i1}	2	10^{-1}	10^{+1}
3	K_{a1}	1	10^{-6}	10^{+6}
4	n_{a1}	2	10^{-1}	10^{+1}
5	k_1	1	10^{-6}	10^{+6}
6	V_2	1	10^{-6}	10^{+6}
7	K_{i2}	1	10^{-6}	10^{+6}
8	n_{i2}	2	10^{-1}	10^{+1}
9	K_{a2}	1	10^{-6}	10^{+6}
10	n_{a2}	2	10^{-1}	10^{+1}
11	k_2	1	10^{-6}	10^{+6}
12	V_3	1	10^{-6}	10^{+6}
13	K_{i3}	1	10^{-6}	10^{+6}
14	n_{i3}	2	10^{-1}	10^{+1}
15	K_{a3}	1	10^{-6}	10^{+6}
16	n_{a3}	2	10^{-1}	10^{+1}
17	k_3	1	10^{-6}	10^{+6}
18	V_4	0.1	10^{-6}	10^{+6}
19	K_4	1	10^{-6}	10^{+6}
20	k_4	0.1	10^{-6}	10^{+6}
21	V_5	0.1	10^{-6}	10^{+6}
22	K_5	1	10^{-6}	10^{+6}
23	k_5	0.1	10^{-6}	10^{+6}
24	V_6	0.1	10^{-6}	10^{+6}
25	K_6	1	10^{-6}	10^{+6}
26	k_6	0.1	10^{-6}	10^{+6}
27	k_{cat1}	1	10^{-6}	10^{+6}
28	K_{m1}	1	10^{-6}	10^{+6}
29	K_{m2}	1	10^{-6}	10^{+6}
30	k_{cat2}	1	10^{-6}	10^{+6}
31	K_{m3}	1	10^{-6}	10^{+6}
32	K_{m4}	1	10^{-6}	10^{+6}
33	k_{cat3}	1	10^{-6}	10^{+6}
34	K_{m5}	1	10^{-6}	10^{+6}
35	K_{m6}	1	10^{-6}	10^{+6}

(a) ODE system

$$\frac{dG_1}{dt} = \frac{V_1}{1 + \left(\frac{P}{K_{i1}}\right)^{n_{i1}} + \left(\frac{K_{a1}}{S}\right)^{n_{a1}}} - k_1 \cdot G_1$$

$$\frac{dG_2}{dt} = \frac{V_2}{1 + \left(\frac{P}{K_{i2}}\right)^{n_{i2}} + \left(\frac{K_{a2}}{M_1}\right)^{n_{a2}}} - k_2 \cdot G_2$$

$$\frac{dG_3}{dt} = \frac{V_3}{1 + \left(\frac{P}{K_{i3}}\right)^{n_{i3}} + \left(\frac{K_{a3}}{M_2}\right)^{n_{a3}}} - k_3 \cdot G_3$$

$$\frac{dE_1}{dt} = \frac{V_4 \cdot G_1}{K_4 + G_1} - k_4 \cdot E_1$$

$$\frac{dE_2}{dt} = \frac{V_5 \cdot G_2}{K_5 + G_2} - k_5 \cdot E_2$$

$$\frac{dE_3}{dt} = \frac{V_6 \cdot G_3}{K_6 + G_3} - k_6 \cdot E_3$$

$$\frac{dM_1}{dt} = \frac{k_{cat1} \cdot E_1 \cdot \frac{1}{K_{m1}} \cdot (S - M_1)}{1 + \frac{S}{K_{m1}} + \frac{M_1}{K_{m2}}}$$
$$- \frac{k_{cat2} \cdot E_2 \cdot \frac{1}{K_{m3}} \cdot (M_1 - M_2)}{1 + \frac{M_1}{K_{m3}} + \frac{M_2}{K_{m4}}}$$

$$\frac{dM_2}{dt} = \frac{k_{cat2} \cdot E_2 \cdot \frac{1}{K_{m3}} \cdot (M_1 - M_2)}{1 + \frac{M_1}{K_{m3}} + \frac{M_2}{K_{m4}}}$$
$$- \frac{k_{cat3} \cdot E_3 \cdot \frac{1}{K_{m5}} \cdot (M_2 - P)}{1 + \frac{M_2}{K_{m5}} + \frac{P}{K_{m6}}}$$

(b) Initial values

G_1	0.66667
G_2	0.57254
G_3	0.41758
E_1	0.4
E_2	0.36409
E_3	0.29457
M_1	1.419
M_2	0.93464

(d) Experimental settings

S	0.1	0.46416	2.1544	10
P	0.05	0.13572	0.3684	1

Table 1. Three-step metabolic pathway. (a) ODE system for the concentrations of mRNAs G_1, G_2, G_3, enzymes E_1, E_2, E_3, and metabolites M_1, M_2. (b) Initial values of the ODE variables. (c) List of parameters: true values, q_*, for generating the experimental data; lower and upper bounds, q_{lb} and q_{ub}. (d) Experimental settings: 4 concentrations of substrate and product, S and P respectively, for generating $4 \times 4 = 16$ experimental data sets.
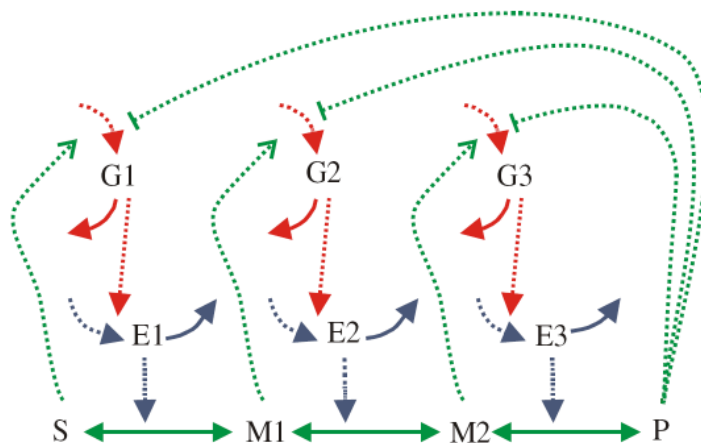
Figure 32. Three-step metabolic pathway (reproduced from [113]). Solid arrows represent mass flow, and dashed arrows represent regulation, where → denotes activation and ⊣ denotes inhibition. Three genes are producing mRNAs G1, G2, G3 and enzymes E1, E2, E3 to regulate the transformation of substrate S into product P via the intermediate metabolites M1, M2.

for generating $4 \times 4 = 16$ experimental data sets, cf. Table 1(d).

For the standardized description of biochemical reaction networks (as in Figure 32) a Systems Biology Markup Language (SBML) has been developed as a community effort [73]. Starting from SBML models the software package SOSlib [107] which we used for our computations generates and solves the ODEs and also contains a parameter identification module; for the fast computation of gradients with respect to unknown parameters, adjoint methods are used [106].

Appendix C

In this Appendix, we present the G_1/S transition model of the cell cycle [149], which is used in the inverse bifurcation analysis of Section 3.2.1. The model includes the following proteins that are involved in the progression from the G_1 to S phase of the cell cycle:

- pRB, pRB_p, pRB_{pp}: retinoblastoma and its phosphorylated forms
- E2F1: transcription factor that target genes regulating cell cycle progression
- CycD_a, CycD_i, CycE_i, CycE_a: cyclin complexes whose concentrations undergo cyclic variations within the cell cycle

The ODE system given below models the interaction of genes involved in the G_1/S module. One major step in the cell cycle is a phosphorylation reaction catalyzed by the CycD_a-dependent kinase, whereby a phosphate group is transferred from ATP to pRB. In the framework presented in Appendix A, pRB and ATP play the role of substrates **A** and **B**, whereas CycD_a (when complexed with a kinase) plays the role of enzyme **E**. The catalyzed reaction yields pRB_p, i.e. the product **C**.

Under the assumption that ATP and kinase are available in abundance, the reaction rate can be approximated by the term $k_{16} \cdot \text{pRB}(t) \cdot \text{CycD}_a(t)$, i.e. by the use of second-order kinetics. This approximation is preferred since using a detailed reaction mechanism and mass-action kinetics for every reaction step – as outlined in Appendix A – results in either a complicated (Michaelis-Menten type) expression for the rate law or a substantial increase in the number of ODEs.

$$\frac{d}{dt}\mathrm{pRB}(t) = \frac{\mathrm{E2F1}(t)J_{11}J_{61}k_1}{(\mathrm{pRB}(t)+J_{11})\left(\mathrm{E2F1}(t)+K_{\mathrm{m1}}\right)\left(J_{61}+\mathrm{pRB}_p(t)\right)}$$

$$\qquad - \mathbf{k_{16}pRB(t)CycD_a(t)} + k_{61}\mathrm{pRB}_p(t) - \mathrm{pRB}(t)\phi_{\mathrm{pRM}}$$

$$\frac{d}{dt}\mathrm{E2F1}(t) = k_p + \frac{\left(a^2+\mathrm{E2F1}(t)^2\right)J_{12}J_{62}k_2}{(\mathrm{pRB}(t)+J_{12})\left(\mathrm{E2F1}(t)^2+K_{\mathrm{m2}}^2\right)\left(J_{62}+\mathrm{pRB}_p(t)\right)} - \phi_{\mathrm{E2F1}}\mathrm{E2F1}(t)$$

$$\frac{d}{dt}\mathrm{CycD}_i(t) = \mathrm{AP1}(t)k_3 + k_{43}\mathrm{CycD}_a(t) - \frac{k_{34}\mathrm{CycD}_a(t)\mathrm{CycD}_i(t)}{K_{\mathrm{m4}}+\mathrm{CycD}_a(t)} - \phi_{\mathrm{CycD}_i}\mathrm{CycD}_i(t)$$

$$\qquad + \frac{\mathrm{E2F1}(t)J_{13}J_{63}k_{23}}{(\mathrm{pRB}(t)+J_{13})\left(J_{63}+\mathrm{pRB}_p(t)\right)}$$

$$\frac{d}{dt}\mathrm{CycD}_a(t) = -k_{43}\mathrm{CycD}_a(t) + \frac{k_{34}\mathrm{CycD}_i(t)\mathrm{CycD}_a(t)}{K_{\mathrm{m4}}+\mathrm{CycD}_a(t)} - \phi_{\mathrm{CycD}_a}\mathrm{CycD}_a(t)$$

$$\frac{d}{dt}\mathrm{AP1}(t) = F_m + \frac{\mathrm{E2F1}(t)J_{15}J_{65}k_{25}}{(\mathrm{pRB}(t)+J_{15})\left(J_{65}+\mathrm{pRB}_p(t)\right)} - \mathrm{AP1}(t)\phi_{\mathrm{AP1}}$$

$$\frac{d}{dt}\mathrm{pRB}_p(t) = \mathbf{k_{16}pRB(t)CycD_a(t)} - k_{61}\mathrm{pRB}_p(t) - k_{67}\mathrm{CycE}_a(t)\mathrm{pRB}_p(t)$$

$$\qquad + k_{76}\mathrm{pRB}_{\mathrm{pp}}(t) - \phi_{\mathrm{pRB}_p}\mathrm{pRB}_p(t)$$

$$\frac{d}{dt}\mathrm{pRB}_{\mathrm{pp}}(t) = k_{67}\mathrm{CycE}_a(t)\mathrm{pRB}_p(t) - k_{76}\mathrm{pRB}_{\mathrm{pp}}(t) - \phi_{\mathrm{pRB}_{pp}}\mathrm{pRB}_{\mathrm{pp}}(t)$$

$$\frac{d}{dt}\mathrm{CycE}_i(t) = \frac{\mathrm{E2F1}(t)J_{18}J_{68}k_{28}}{(\mathrm{pRB}(t)+J_{18})\left(J_{68}+\mathrm{pRB}_p(t)\right)}$$

$$\qquad + k_{98}\mathrm{CycE}_a(t) - \frac{k_{89}\mathrm{CycE}_a(t)\mathrm{CycE}_i(t)}{K_{\mathrm{m9}}+\mathrm{CycE}_a(t)} - \phi_{\mathrm{CycE}_i}\mathrm{CycE}_i(t)$$

$$\frac{d}{dt}\mathrm{CycE}_a(t) = -k_{98}\mathrm{CycE}_a(t) + \frac{k_{89}\mathrm{CycE}_i(t)\mathrm{CycE}_a(t)}{K_{\mathrm{m9}}+\mathrm{CycE}_a(t)} - \phi_{\mathrm{CycE}_a}\mathrm{CycE}_a(t)$$

Appendix D

The following is the ODE system of the circadian rhythm model [149] which is used in the inverse analysis of Section 3.2.3.

$$\frac{d}{dt}C_c(t) = -k_1C_c(t) - k_4C_c(t) - k_{\mathrm{dC}}C_c(t) + k_2C_n(t) + k_3P_2(t)T_2(t)$$

$$\frac{d}{dt}C_n(t) = k_1C_c(t) - k_2C_n(t) - k_{\mathrm{dN}}C_n(t)$$

$$\frac{d}{dt}M_p(t) = \frac{V_{\mathrm{sP}}K_{\mathrm{IP}}^n}{K_{\mathrm{IP}}^n+C_n(t)^n} - k_dM_p(t) - \frac{v_{\mathrm{mP}}M_p(t)}{K_{\mathrm{mP}}+M_p(t)}$$

$$\frac{d}{dt}M_t(t) = \frac{v_{\mathrm{sT}}K_{\mathrm{IT}}^n}{K_{\mathrm{IT}}^n+C_n(t)^n} - k_dM_t(t) - \frac{v_{\mathrm{mT}}M_t(t)}{K_{\mathrm{mT}}+M_t(t)}$$

$$\frac{d}{dt}P_0(t) = k_{\mathrm{sP}}M_p(t) - k_dP_0(t) - \frac{V_PP_0(t)}{K_P+P_0(t)} + \frac{V_{2P}P_1(t)}{K_{2P}+P_1(t)}$$

$$\frac{d}{dt}P_1(t) = \frac{V_PP_0(t)}{K_P+P_0(t)} - k_dP_1(t) - \frac{V_{2P}P_1(t)}{K_{2P}+P_1(t)} - \frac{V_{3P}P_1(t)}{K_{3P}+P_1(t)} + \frac{V_{4P}P_2(t)}{K_{4P}+P_2(t)}$$

$$\frac{d}{dt}P_2(t) = k_4C_c(t) - k_dP_2(t) - k_3P_2(t)T_2(t) + \frac{V_{3P}P_1(t)}{K_{3P}+P_1(t)} - \frac{V_{\mathrm{dP}}P_2(t)}{K_{\mathrm{dP}}+P_2(t)} - \frac{V_{4P}P_2(t)}{K_{4P}+P_2(t)}$$

$$\frac{d}{dt}T_0(t) = k_{\mathrm{sT}}M_t(t) - k_dT_0(t) - \frac{V_TT_0(t)}{K_T+T_0(t)} + \frac{V_{2T}T_1(t)}{K_{2T}+T_1(t)}$$

$$\frac{d}{dt}T_1(t) = \frac{V_TT_0(t)}{K_T+T_0(t)} - k_dT_1(t) - \frac{V_{2T}T_1(t)}{K_{2T}+T_1(t)} - \frac{V_{3T}T_1(t)}{K_{3T}+T_1(t)} + \frac{V_{4T}T_2(t)}{K_{4T}+T_2(t)}$$

$$\frac{d}{dt}T_2(t) = k_4C_c(t) - k_dT_2(t) - k_3P_2(t)T_2(t) + \frac{V_{3T}T_1(t)}{K_{3T}+T_1(t)} - \frac{V_{\mathrm{dT}}T_2(t)}{K_{\mathrm{dT}}+T_2(t)} - \frac{V_{4T}T_2(t)}{K_{4T}+T_2(t)}$$

[1] S. O. Aase and P. Ruoff. Semi-algebraic optimization of temperature compensation in a general switch-type negative feedback model of circadian clocks. *J Math Biol*, 56:279–292, Mar 2008.

[2] U. Alon. Network motife: theory and experimental approaches. *Nature Reviews Genetics*, 8:450–461, 2007.

[3] P. Aloy and R. B. Russell. Structural systems biology: modelling protein interactions. *Nature Reviews Mol. Cellbiol.*, 7:188–197, 2006.

[4] E. Andrianantoandro, S. Basu, D. K. Karig, and R. Weiss. Synthetic biology: new engineering rules for an emerging discipline. *Mol Syst Biol*, 2:2006.0028, 2006.

[5] A. Arkin and J. Ross. Statistical construction of chemical reaction mechanisms from measured time-series. *The Journal of Physical Chemistry*, 99(3):970–979, 1995.

[6] A. B. Bakushinskiĭ. On a convergence problem of the iterative-regularized Gauss-Newton method. *Zh. Vychisl. Mat. i Mat. Fiz.*, 32(9):1503–1509, 1992.

[7] A. Bakushinsky and M. Kokurin. *Iterative Methods for Approximate Solution of Inverse Problems*, volume 577 of *Mathematics and its Applications*. Springer, Dordrecht, 2004.

[8] A. L. Barabási and Z. N. Oltvai. Network biology: understanding the cell's functional organization. *Nat Rev Genet*, 5(2):101–13, Feb 2004.

[9] D. M. Bates and D. G. Watts. *Nonlinear Regression Analysis and its Applications*. Wiley Series in Probability and Mathematical Statistics. John Wiley & Sons, Inc., 1988.

[10] F. Bauer, T. Hohage, and A. Munk. Iteratively regularized Gauss-Newton method for nonlinear inverse problems with random noise. *SIAM J. Numer. Anal.*, 47(3):1827–1846, 2009.

[11] F. Bauer, S. Pereverzyev, and L. Rosasco. On regularization algorithms in learning theory. *Journal of Complexity*, 23:52–72, 2007.

[12] N. Bissantz, T. Hohage, A. Munk, and F. H. Ruymgaart. Convergence rates of general regularization methods for statistical inverse problems and applications. *SIAM J. Numer. Anal.*, 45:2610–2636, 2007.

[13] B. Blaschke, A. Neubauer, and O. Scherzer. On convergence rates for the iteratively regularized Gauss-Newton method. *IMA J. Numer. Anal.*, 17(3):421–436, 1997.

[14] H. G. Bock. Numerical treatment of inverse problems in chemical reaction kinetics. In *Modelling of Chemical Reaction Systems*, pages 102–125. Springer, Berlin, Heidelberg, New York, 1981.

[15] H. G. Bock. Randwertproblemmethoden zur Parameteridentifizierung in Systemen nichtlinearer Differentialgleichungen. *Bonner Mathematische Schriften*, 183, 1987.

[16] B. Canton, A. Labno, and D. Endy. Refinement and standardization of synthetic biological parts and devices. *Nat Biotechnol*, 26(7):787–93, Jul 2008.

[17] A. Chatterjee, Y. N. Kaznessis, and W. S. Hu. Tweaking biological switches through a better understanding of bistability behavior. *Curr. Opin. Biotechnol.*, 19:475–481, Oct 2008.

[18] T. Chevalier, I. Schreiber, and J. Ross. Toward a systematic determination of complex reaction mechanisms. *The Journal of Physical Chemistry*, 97(26):6776–6787, 1993.

[19] V. Chickarmane, S. R. Paladugu, F. Bergmann, and H. M. Sauro. Bifurcation discovery tool. *Bioinformatics*, 21:3688–3690, Sep 2005.

[20] I.-C. Chou, H. Martens, and E. O. Voit. Parameter estimation in biochemical systems models with alternating regression. *Theor Biol Med Model*, 3:25, 2006.

[21] I.-C. Chou and E. O. Voit. Recent developments in parameter estimation and structure identification of biochemical and genomic systems. *Mathematical Biosciences*, 219(2):57–83, 2009.

[22] B. L. Clarke. Stoichiometric network analysis. *Cell Biophys.*, 12:237–253, 1988.

[23] E. Conrad. *Bifurcation Analysis and qualitative optimization of models in molecular cell biology with applications to the circadian clock*. PhD in Mathematics, Virginia Polytechnic Institute and State University, 2006.

[24] A. Cornish-Bowden. *Fundamentals of Enzyme Kinetics*. Portland Press, third edition, 2004.

[25] G. Craciun, Y. Tang, and M. Feinberg. Understanding bistability in complex enzyme-driven reaction networks. *Proc Natl Acad Sci USA*, 103(23):8697–702, Jun 2006.

[26] A. Csikász-Nagy, D. Battogtokh, K. C. Chen, B. Novák, and J. J. Tyson. Analysis of a generic model of eukaryotic cell-cycle regulation. *Biophys. J.*, 90:4361–4379, Jun 2006.

[27] A. d'Aspremont, L. El Ghaoui, M. I. Jordan, and G. R. G. Lanckriet. A direct formulation for sparse PCA using semidefinite programming. *SIAM Rev.*, 49(3):434–448 (electronic), 2007.

[28] I. Daubechies, M. Defrise, and C. De Mol. An iterative thresholding algorithm for linear inverse problems with a sparsity constraint. *Comm. Pure Appl. Math.*, 57(11):1413–1457, 2004.

[29] H. de Jong. Modeling and simulation of genetic regulatory systems: a literature review. *J Comput Biol*, 9(1):67–103, 2002.

[30] H. de Jong, J. Gouze, C. Hernandez, M. Page, T. Sari, and J. Geiselmann. Qualitative simulation of genetic regulatory networks using piecewise-linear models. *Bulletin of Mathematical Biology*, 66(2):301–340, 2004.

[31] P. Deuflhard, H. W. Engl, and O. Scherzer. A convergence analysis of iterative methods for the solution of nonlinear ill-posed problems under affinely invariant conditions. *Inverse Problems*, 14:1081–1106, 1998.

[32] A. Dhooge, W. Govaerts, Y. A. Kuznetsov, H. G. E. Meijer, and B. Sautois. New features of the software MatCont for bifurcation analysis of dynamical systems. *Math. Comput. Model. Dyn. Syst.*, 14(2):147–175, 2008.

[33] I. Dobson. Computing a closest bifurcation instability in multidimensional parameter space. *J. Nonlinear Sci.*, 3(3):307–327, 1993.

[34] E. Doedel. AUTO: a program for the automatic bifurcation analysis of autonomous systems. In *Proceedings of the Tenth Manitoba Conference on Numerical Mathematics and Computing, Vol. I (Winnipeg, Man., 1980)*, volume 30, pages 265–284, 1981.

[35] P. P. B. Eggermont. Maximum entropy regularization for Fredholm integral equations of the first kind. *SIAM J. Math. Anal.*, 24(6):1557–1576, 1993.

[36] L. Endler, N. Rodriguez, N. Juty, V. Chelliah, C. Laibe, C. Li, and N. Le Novre. Designing and encoding models for synthetic biology. *J R Soc Interface*, 6 Suppl 4:S405–417, Aug 2009.

[37] H. W. Engl and W. Grever. Using the *L*-curve for determining optimal regularization parameters. *Numer. Math.*, 69(1):25–31, 1994.

[38] H. W. Engl, M. Hanke, and A. Neubauer. *Regularization of inverse problems*, volume 375 of *Mathematics and its Applications*. Kluwer Academic Publishers Group, Dordrecht, 1996.

[39] H. W. Engl, A. Hofinger, and S. Kindermann. Convergence rates in the Prokhorov metric for assessing uncertainty in ill-posed problems. *Inverse Problems*, 21:399–412, 2005.

[40] H. W. Engl, K. Kunisch, and A. Neubauer. Convergence rates for Tikhonov regularisation of nonlinear ill-posed problems. *Inverse Problems*, 5(4):523–540, 1989.

[41] H. W. Engl and G. Landl. Convergence rates for maximum entropy regularization. *SIAM J. Numer. Anal.*, 30(5):1509–1536, 1993.

[42] H. W. Engl and G. Landl. Maximum entropy regularization of nonlinear ill-posed problems. In *World Congress of Nonlinear Analysts '92, Vol. I–IV (Tampa, FL, 1992)*, pages 513–525. de Gruyter, Berlin, 1996.

[43] H. W. Engl and O. Scherzer. Convergence rates results for iterative methods for solving nonlinear ill-posed problems. In *Surveys on solution methods for inverse problems*, pages 7–34. Springer, Vienna, 2000.

[44] C. P. Fall, E. S. Marland, J. M. Wagner, and J. J. Tyson, editors. *Computational Cell Biology*, volume 20 of *Interdisciplinary Applied Mathematics*. Springer-Verlag, New York, 2002.

[45] M. Feinberg. Complex balancing in general kinetic systems. *Arch. Rational Mech. Anal.*, 49:187–194, 1972.

[46] M. Feinberg and F. J. M. Horn. Dynamics of open chemical systems and the algebraic structure of the underlying reaction network. *Chem. Eng. Sci.*, 29(3):775–787, 1973.

[47] D. A. Fell. *Understanding the Control of Metabolism*. Portland Press, London, 1997.

[48] J. Gagneur and S. Klamt. Computation of elementary modes: a unifying framework and the new binary approach. *BMC Bioinformatics*, 5:175 [epub], 2004.

[49] P. Gennemark and D. Wedelin. Efficient algorithms for ordinary differential equation model identification of biological systems. *IET Syst Biol*, 1(2):120–9, 2007.

[50] L. Glass. Classification of biological networks by their qualitative dynamics. *J Theor Biol*, 54(1):85–107, 1975.

[51] L. Glass and M. C. Mackey. Pathological conditions resulting from instabilities in physiological control systems. *Ann. N. Y. Acad. Sci.*, 316:214–235, 1979.

[52] W. Govaerts, Y. A. Kuznetsov, and A. Dhooge. Numerical continuation of bifurcations of limit cycles in MATLAB. *SIAM J. Sci. Comput.*, 27(1):231–252, 2005.

[53] W. Govaerts, Y. A. Kuznetsov, and B. Sijnave. Continuation of codimension-2 equilibrium bifurcations in CONTENT. In *Numerical methods for bifurcation problems and large-scale dynamical systems (Minneapolis, MN, 1997)*, volume 119 of *IMA Vol. Math. Appl.*, pages 163–184. Springer, New York, 2000.

[54] W. J. F. Govaerts. *Numerical Methods for Bifurcations of Dynamical Equilibria*. Society for Industrial and Applied Mathematics (SIAM), Philadelphia, PA, 2000.

[55] M. Grasmair, M. Haltmeier, and O. Scherzer. Sparse regularization with l^q penalty term. *Inverse Problems*, 24(5):055020, 2008.

[56] R. Griesse and D. A. Lorenz. A semismooth Newton method for Tikhonov functionals with sparsity constraints. *Inverse Problems*, 24(3):035007, 19pp, 2008.

[57] J. M. Guberman. Mass action networks and the deficiency zero theorem. Master's thesis, Department of Mathematics, Harvard University, 2003.

[58] R. Gunawan, K. G. Gadkar, and F. J. Doyle. Methods to identify cellular architecture and

dynamics from experimental data. In Z. Szallasi, J. Stelling, and V. Periwal, editors, *System Modeling in Cellular Biology: From Concepts to Nuts and Bolts*, pages 179–183. MIT Press, Boston, 2006.

[59] J. Gunawardena. Chemical reaction network theory for in-silico biologists. Technical report, `http://vcp.med.harvard.edu/papers/crnt.pdf`, 2003.

[60] S. Gupta, E. Aslakson, B. M. Gurbaxani, and S. D. Vernon. Inclusion of the glucocorticoid receptor in a hypothalamic pituitary adrenal axis model reveals bistability. *Theor Biol Med Model*, 4:8, 2007.

[61] R. N. Gutenkunst, J. J. Waterfall, F. P. Casey, K. S. Brown, C. R. Myers, and J. P. Sethna. Universally sloppy parameter sensitivities in systems biology models. *PLoS Comput Biol*, 3(10):1871–78, 2007.

[62] M. Hanke. A regularizing Levenberg-Marquardt scheme, with applications to inverse groundwater filtration problems. *Inverse Problems*, 13(1):79–95, 1997.

[63] M. Hanke and P. C. Hansen. Regularization methods for large-scale problems. *Surveys Math. Indust.*, 3(4):253–315, 1993.

[64] M. Hanke, A. Neubauer, and O. Scherzer. A convergence analysis of the Landweber iteration for nonlinear ill-posed problems. *Numerische Mathematik*, 72:21–37, 1995.

[65] P. C. Hansen and D. P. O'Leary. The use of the *L*-curve in the regularization of discrete ill-posed problems. *SIAM J. Sci. Comput.*, 14(6):1487–1503, 1993.

[66] R. Heinrich and T. A. Rapoport. A linear steady-state treatment of enzymatic chains. General properties, control and effector strengths. *Eur. J. Biochem.*, 42:97–105, 1974.

[67] R. Heinrich and S. Schuster. *The Regulation of Cellular Systems*. Chapman and Hall, 1996.

[68] A. Hofinger and H. K. Pikkarainen. Convergence rate for the Bayesian approach to linear inverse problems. *Inverse Problems*, 23:2469–2484, 2007.

[69] T. Hohage and M. Pricop. Nonlinear Tikhonov regularization in Hilbert scales for inverse boundary value problems with random noise. *Inverse Probl. Imaging*, 2:271–290, 2008.

[70] C. I. Hong, E. D. Conrad, and J. J. Tyson. A proposal for robust temperature compensation of rhythms. *Proc. Natl. Acad. Sci. U.S.A.*, 104:1195–1200, Jan 2007.

[71] F. Horn. Necessary and sufficient conditions for complex balancing in chemical kinetics. *Arch. Rational Mech. Anal.*, 49:172–186, 1972.

[72] F. Horn and R. Jackson. General mass action kinetics. *Arch. Rational Mech. Anal.*, B47:81–116, 1972.

[73] M. Hucka, A. Finney, H. M. Sauro, H. Bolouri, J. C. Doyle, H. Kitano, A. P. Arkin, B. J. Bornstein, D. Bray, A. Cornish-Bowden, A. A. Cuellar, S. Dronov, E. D. Gilles, M. Ginkel, V. Gor, I. Goryanin, W. J. Hedley, T. C. Hodgman, J. H. Hofmeyr, P. J. Hunter, N. S. Juty, J. L. Kasberger, A. Kremling, U. Kummer, N. Le Novére, L. M. Loew, D. Lucio, P. Mendes, E. Minch, E. D. Mjolsness, Y. Nakayama, M. R. Nelson, P. F. Nielsen, T. Sakurada, J. C. Schaff, B. E. Shapiro, T. S. Shimizu, H. D. Spence, J. Stelling, K. Takahashi, M. Tomita, J. Wagner, J. Wang, and S. Forum. The systems biology markup language (SBML): a medium for representation and exchange of biochemical network models. *Bioinformatics*, 19(4):524–531, Mar 2003.

[74] R. Ibarra, J. Edwards, and B. Palsson. *Escherichia coli* k-12 undergoes adaptive evolution to achieve *in silico* predicted optimal groth. *Nature*, 420:186–189, 2002.

[75] E. M. Izhikevich. *Dynamical systems in neuroscience: the geometry of excitability and bursting*. Computational Neuroscience. MIT Press, Cambridge, MA, 2007.

[76] K. Jaqaman and G. Danuser. Linking data to models: data regression. In A. Heinrichs, E. Kritikou, B. Pulverer, and M. Raftopoulou, editors, *Systems Biology: a User's Guide*, pages 27–33. Nature Publishing, New York, Nov 2006.

[77] H. Jeong, B. Tombor, R. Albert, Z. N. Oltvai, and A. L. Barabasi. The large-scale organization of metabolic networks. *Nature*, 407(6804):651–4, 2000.

[78] X. Ji and Y. Xu. libSRES: a C library for stochastic ranking evolution strategy for parameter estimation. *Bioinformatics*, 22:124–126, Jan 2006.

[79] H. Kacser and J. A. Burns. The control of flux. *Symp. Soc. Exp. Biol.*, 32:65–104, 1973.

[80] H. Kacser, J. A. Burns, and D. A. Fell. The control of flux: 21 years on. *Biochem. Soc. Trans.*, 23:341–366, 1995.

[81] J. Kaipio and E. Somersalo. *Statistical and Computational Inverse Problems*, volume 160 of *Applied Mathematical Sciences*. Springer, New York, 2004.

[82] B. Kaltenbacher, A. Neubauer, and O. Scherzer. *Iterative regularization methods for nonlinear ill-posed problems*, volume 6 of *Radon Series on Computational and Applied Mathematics*. Walter de Gruyter GmbH & Co. KG, Berlin, 2008.

[83] Y. N. Kaznessis. Models for synthetic biology. *BMC Syst Biol*, 1:47, 2007.

[84] P. D. Kepper, J. Boissonade, and I. R. Epstein. Chlorite-iodide reaction: a versatile system for the study of nonlinear dynamic behavior. *Journal of Physical Chemistry*, 94:6525–6536, 1990.

[85] S. Kikuchi, D. Tominaga, M. Arita, K. Takahashi, and M. Tomita. Dynamic modeling of genetic networks using genetic algorithm and S-system. *Bioinformatics*, 19(5):643–50, 2003.

[86] R. R. Klevecz and D. B. Murray. Genome wide oscillations in expression. Wavelet analysis of time series data from yeast expression arrays uncovers the dynamic architecture of phenotype. *Mol. Biol. Rep.*, 28:73–82, 2001.

[87] E. Klipp, R. Herwig, A. Kowald, C. Wierling, and H. Lehrach. *Systems Biology in Practice. Concepts, Implementation, and Application.* Wiley-VCH Verlag, Weinheim, DE, 2005.

[88] A. Kremling, S. Fischer, K. Gadkar, F. J. Doyle, T. Sauter, E. Bullinger, F. Allgöwer, and E. D. Gilles. A benchmark for methods in reverse engineering and model discrimination: problem formulation and solutions. *Genome Res*, 14(9):1773–85, 2004.

[89] P. Kügler, E. Gaubitzer, and S. Müller. Parameter identification for chemical reaction systems using sparsity enforcing regularization: a case study for the chlorite-iodide reaction. *J Phys Chem A*, 113(12):2775–85, 2009.

[90] B. J. Kuipers. Qualitative simulation. *Artif. Intell.*, 29(3):289–338, 1986.

[91] B. J. Kuipers. *Qualitative Reasoning: Modeling and Simulation with Incomplete Knowledge.* MIT Press, 1994.

[92] Y. A. Kuznetsov. *Elements of Applied Bifurcation Theory*, volume 112 of *Applied Mathematical Sciences*. Springer-Verlag, New York, third edition, 2004.

[93] Y. A. Kuznetsov, W. Govaerts, E. J. Doedel, and A. Dhooge. Numerical periodic normalization for codim 1 bifurcations of limit cycles. *SIAM J. Numer. Anal.*, 43(4):1407–1435 (electronic), 2005.

[94] G. Landl and R. S. Anderssen. Non-negative differentially constrained entropy-like regularization. *Inverse Problems*, 12(1):35–53, 1996.

[95] F. Lei and S. B. Jorgensen. Estimation of kinetic parameters in a structured yeast model using regularisation. *J Biotechnol*, 88(3):223–37, 2001.

[96] J. C. Leloup and A. Goldbeter. Temperature compensation of circadian rhythms: control of the period in a model for circadian oscillations of the PER protein in Drosophila. *Chronobiol. Int.*, 14:511–520, Sep 1997.

[97] J. C. Leloup and A. Goldbeter. A model for circadian rhythms in Drosophila incorporating the formation of a complex between the PER and TIM proteins. *J. Biol. Rhythms*, 13:70–87, Feb 1998.

[98] J. C. Leloup and A. Goldbeter. Chaos and birhythmicity in a model for circadian oscillations of the PER and TIM proteins in Drosophila. *J. Theor. Biol.*, 198:445–459, Jun 1999.

[99] J. C. Leloup and A. Goldbeter. Modeling the circadian clock: from molecular mechanism to physiological disorders. *Bioessays*, 30:590–600, Jun 2008.

[100] C. M. Li and R. R. Klevecz. A rapid genome-scale response of the transcriptional oscillator to perturbation reveals a period-doubling path to phenotypic change. *Proc. Natl. Acad. Sci. U.S.A.*, 103:16254–16259, Oct 2006.

[101] W. Liebermeister and E. Klipp. Bringing metabolic networks to life: convenience rate law and thermodynamic constraints. *Theor Biol Med Model*, 3:41, 2006.

[102] J. C. Locke, L. Kozma-Bognr, P. D. Gould, B. Fehr, E. Kevei, F. Nagy, M. S. Turner, A. Hall, and A. J. Millar. Experimental validation of a predicted feedback loop in the multi-oscillator clock of Arabidopsis thaliana. *Mol. Syst. Biol.*, 2:59, 2006.

[103] J. Lu. Inverse eigenvalue problems for exploring the dynamics of systems biology models. *Advances in Applied Mathematics and Mechanics*, 1:711–728, 2009.

[104] J. Lu, H. W. Engl, R. Machné, and P. Schuster. Inverse bifurcation analysis of a model for mammalian G_1/S regulatory module. In *BIRD '07*, volume 4414 of *Lecture Notes in Bioinformatics*, pages 168–184. Springer, 2007.

[105] J. Lu, H. W. Engl, and P. Schuster. Inverse bifurcation analysis: application to simple gene systems. *Algorithms Mol Biol*, 1:11, 2006.

[106] J. Lu, S. Müller, R. Machné, and C. Flamm. SBML ODE Solver library: Extensions for inverse analysis. In *Proceedings of the Fifth International Workshop on Computational Systems Biology, WCSB 2008, Leipzig, Germany*, 2008.

[107] R. Machné, A. Finney, S. Müller, J. Lu, S. Widder, and C. Flamm. The SBML ODE Solver Library: a native API for symbolic and fast numerical analysis of reaction networks. *Bioinformatics*, 22(11):1406–7, 2006.

[108] F. Marcus. *Bioinformatics and Systems Biology.* Springer-Verlag, Berlin, 2008.

[109] R. Milo, S. Shen-Orr, S. Itzkovitz, N. Kashtan, D. Chklovskii, and U. Alon. Network motifs: simple building blocks of complex networks. *Science*, 298(5594):824–7, 2002.

[110] M. Mincheva and M. R. Roussel. A graph-theoretical method for detecting potential turing bifurcations. *J. Chem. Phys.*, 125:204102, 2006.

[111] M. Mincheva and M. R. Roussel. Graph-theoretic methods for the analysis of chemical and biochemical networks. I. Multistability and oscillations in ordinary differential equation models. *J Math Biol*, 55(1):61–86, Jul 2007.

[112] M. Mincheva and M. R. Roussel. Graph-theoretic methods for the analysis of chemical and biochemical networks. II. Oscillations in networks with delays. *J Math Biol*, 55(1):87–104, Jul 2007.

[113] C. G. Moles, P. Mendes, and J. R. Banga. Parameter estimation in biochemical pathways: a comparison of global optimization methods. *Genome Res*, 13(11):2467–74, 2003.

[114] M. Mönnigmann and W. Marquardt. Normal vectors on manifolds of critical points for parametric robustness of equilibrium solutions of ODE systems. *J. Nonlinear Sci.*, 12(2):85–112, 2002.

[115] S. Müller, J. Hofbauer, L. Endler, C. Flamm, S. Widder, and P. Schuster. A generalized model of the repressilator. *J. Math. Biol.*, 53(6):905–937, 2006.

[116] M. Z. Nashed and O. Scherzer. Least squares and bounded variation regularization with nondifferentiable functionals. *Numer. Funct. Anal. Optim.*, 19(7-8):873–901, 1998.

[117] A. Neubauer. Tikhonov regularisation for nonlinear ill-posed problems: optimal convergence rates and finite-dimensional approximation. *Inverse Problems*, 5(4):541–557, 1989.

[118] A. Neubauer and H. Pikkarainen. Convergence results for the Bayesian inversion theory. *J. Inv. Ill-Posed Problems*, 16:601–613, 2008.

[119] A. Ng, B. Bursteinas, Q. Gao, E. Mollison, and M. Zvelebil. Resources for integrative systems biology: from data through databases to networks and dynamic system models. *Brief Bioinform*, 7(4):318–30, Dec 2006.

[120] B. Novák and J. J. Tyson. Design principles of biochemical oscillators. *Nat. Rev. Mol. Cell Biol.*, 9:981–991, Dec 2008.

[121] U. Nowak and P. Deuflhard. Numerical identification of selected rate constants in large chemical reaction systems. *Appl. Num. Math.*, 1:59–75, 1985.

[122] N. D. Price, J. L. Reed, and B. Ø. Palsson. Genome-scale models of microbial cells: evaluating the consequences of constraints. *Nature Review Micobiol*, 2:886–897, 2004.

[123] R. Ramlau and G. Teschke. A Tikhonov-based projection iteration for nonlinear ill-posed problems with sparsity constraints. *Numer. Math.*, 104(2):177–203, 2006.

[124] D. A. Rand, B. V. Shulgin, D. Salazar, and A. J. Millar. Design principles underlying circadian clocks. *J R Soc Interface*, 1:119–130, Nov 2004.

[125] D. A. Rand, B. V. Shulgin, J. D. Salazar, and A. J. Millar. Uncovering the design principles of circadian clocks: mathematical analysis of flexibility and evolutionary goals. *J. Theor. Biol.*, 238:616–635, Feb 2006.

[126] M. Rodriguez-Fernandez, J. A. Egea, and J. R. Banga. Novel metaheuristic for parameter estimation in nonlinear dynamic biological systems. *BMC Bioinformatics*, 7:483, 2006.

[127] M. Rodriguez-Fernandez, P. Mendes, and J. R. Banga. A hybrid approach for efficient and robust parameter estimation in biochemical pathways. *Biosystems*, 83(2-3):248–65, 2006.

[128] J. Ross. From the determination of complex reaction mechanisms to systems biology. *Annual Review of Biochemistry*, 77:479–494, 2008.

[129] M. Rowland and T. N. Tozer. *Clinical Pharmacokinetics: Concepts and Applications.* Lippincott, Williams & Wilkins, Philadelphia, PA, 1995.

[130] L. Rudin and S. Osher. Total variation based restoration with free local constraints. In *Proc. of IEEE Int. Conf. on Image Processing, Austin, Texas*, pages 31–35, 1994.

[131] P. Ruoff, M. K. Christensen, and V. K. Sharma. PER/TIM-mediated amplification, gene dosage effects and temperature compensation in an interlocking-feedback loop model of the Drosophila circadian clock. *J. Theor. Biol.*, 237:41–57, Nov 2005.

[132] P. Ruoff, M. Zakhartsev, and H. V. Westerhoff. Temperature compensation through systems biology. *FEBS J.*, 274:940–950, Feb 2007.

[133] M. Sabouri-Ghomi, A. Ciliberto, S. Kar, B. Novak, and J. J. Tyson. Antagonism and bistability in protein interaction networks. *J Theor Biol*, 250(1):209–18, 2008.

[134] U. Sauer. Metabolic networks in motion: ^{13}C-based flux analysis. *Mol. Syst. Biol*, 2:62, 2006.

[135] M. A. Savageau. Biochemical systems analysis. I. Some mathematical properties of the rate law for the component enzymatic reactions. *J Theor Biol*, 25(3):365–9, 1969.

[136] M. A. Savageau. Biochemical systems analysis. II. The steady-state solutions for an n-pool system using a power-law approximation. *J Theor Biol*, 25(3):370–9, 1969.

[137] M. A. Savageau. Biochemical systems analysis. 3. Dynamic solutions using a power-law approximation. *J Theor Biol*, 26(2):215–26, 1970.

[138] M. A. Savageau. Are there rules governing patterns of gene regulation? In B. Goodwin and P. Saunders, editors, *Theoretical Biology; Epigenetic and Evolutionary Order from Complex Systems*, pages 42–66. Edinburgh University Press, 1989.

[139] M. A. Savageau. A kinetic formalism for integrative molecular biology. In B. Magasanik, J. Collado, and T. Smith, editors, *Integrative Approaches to Molecular Biology*, pages 115–146. MIT Press, 1996.

[140] O. Scherzer. Explicit versus implicit relative error regularization on the space of functions of bounded variation. In *Inverse problems, image analysis, and medical imaging (New Orleans, LA, 2001)*, volume 313 of *Contemp. Math.*, pages 171–198. Amer. Math. Soc., Providence, RI, 2002.

[141] C. H. Schilling, D. Letscher, and B. Ø. Palsson. Theory for the systematic definition of metabolic pathways and their use in interpreting metabolic function from a pathway-oriented perspective. *J. Theor. Biol.*, 203:229–248, 2000.

[142] C. H. Schilling and B. Ø. Palsson. The underlying pathway structure of biochemical reaction networks. *Proc. Natl. Acad. Sci. USA*, 95:4193–4198, 1998.

[143] S. Schuster, T. Dandekar, and D. A. Fell. Detection of elementary flux modes in biochemical networks: a promising tool for pathway analysis and metabolic engineering. *Trends Biotechnol*, 17(2):53–60, 1999.

[144] S. Schuster, D. A. Fell, and T. Dandekar. A general definition of metabolic pathways useful for systematic organization and analysis of complex metabolic networks. *Nature Biotechnol.*, 18:326–332, 2000.

[145] P. H. Sellers. An Introduction to a Mathematical Theory of Chemical Reaction Networks I & II. *Arch. Rat. Mech. Anal.*, 44:23–40, 376–386, 1971/1972.

[146] R. P. Shetty, D. Endy, and T. F. Knight. Engineering BioBrick vectors from BioBrick parts. *J Biol Eng*, 2:5, 2008.

[147] N. Soranzo and C. Altafini. ERNEST: a toolbox for chemical reaction network theory. *Bioinformatics*, 25(21):2853–4, 2009.

[148] J. Stelling, S. Klampt, K. Bettenbrock, S. Schuster, and E. Gilles. Metabolic network structure determines key aspects of functionality and regulation. *Nature*, 420:190–193, 2002.

[149] M. Swat, A. Kel, and H. Herzel. Bifurcation analysis of the regulatory modules of the mammalian G_1/S transition. *Bioinformatics*, 20(10):1506–1511, Jul 2004.

[150] Y. J. Tang, H. G. Martin, S. Myers, S. Rodriguez, E. E. Baidoo, and J. D. Keasling. Advances in analysis of microbial metabolic fluxes via ^{13}C isotopic labeling. *Mass Spectrom Rev*, 28(2):362–75, 2009.

[151] M. Terzer and J. Stelling. Large-scale computation of elementary flux modes with bit pattern trees. *Bioinformatics*, 24(19):2229–35, Oct 2008.

[152] B. Teusink, J. Passarge, C. A. Reijenga, E. Esgalhado, C. C. van der Weijden, M. Schepper, M. C. Walsh, B. M. Bakker, K. van Dam, H. V. Westerhoff, and J. L. Snoep. Can yeast glycolysis be understood in terms of in vitro kinetics of the constituent enzymes? Testing biochemistry. *Eur J Biochem*, 267(17):5313–29, Sep 2000.

[153] R. Thomas and M. Kaufman. Multistationarity, the basis of cell differentiation and memory. I. Structural conditions of multistationarity and other nontrivial behavior. *Chaos*, 11(1):170–179, 2001.

[154] J. J. Tyson. Bringing cartoons to life. *Nature*, 445:823, Feb 2007.

[155] J. J. Tyson, K. Chen, and B. Novak. Network dynamics and cell physiology. *Nat. Rev. Mol. Cell Biol.*, 2:908–916, Dec 2001.

[156] J. J. Tyson, K. C. Chen, and B. Novak. Sniffers, buzzers, toggles and blinkers: dynamics of regulatory and signaling pathways in the cell. *Curr. Opin. Cell Biol.*, 15:221–231, Apr 2003.

[157] W. Vance, A. Arkin, and J. Ross. Determination of causal connectivities of species in reaction networks. *Proc Natl Acad Sci USA*, 99(9):5816–21, 2002.

[158] C. R. Vogel. Non-convergence of the L-curve regularization parameter selection method. *Inverse Problems*, 12(4):535–547, 1996.

[159] G. Wahba. *Spline models for observational data*, volume 59 of *CBMS-NSF Regional Conference Series in Applied Mathematics*. Society for Industrial and Applied Mathematics (SIAM), Philadelphia, PA, 1990.

[160] S. Widder, J. Schicho, and P. Schuster. Dynamic patterns of gene regulation I: simple two-gene systems. *J Theor Biol*, 246(3):395–419, 2007.

[161] J. Yan, B. M. Barnes, F. Kohl, and T. G. Marr. Modulation of gene expression in hibernating arctic ground squirrels. *Physiol. Genomics*, 32:170–181, Jan 2008.

[162] J. Yan, A. Burman, C. Nichols, L. Alila, L. C. Showe, M. K. Showe, B. B. Boyer, B. M. Barnes, and T. G. Marr. Detection of differential gene expression in brown adipose tissue of hibernating arctic ground squirrels with mouse microarrays. *Physiol. Genomics*, 25:346–353, Apr 2006.

[163] C. Zarzer. On Tikhonov regularization with non-convex sparsity constraints. *Inverse Problems*, 25(2):025006, 2009.

[164] Z. Zi and E. Klipp. SBML-PET: a Systems Biology Markup Language-based parameter estimation tool. *Bioinformatics*, 22:2704–2705, Nov 2006.